Efficient quantum state preparation with Walsh series

Julien Zylberman and Fabrice Debbasch
LERMA, CNRS, Sorbonne Université, Observatoire de Paris, Université PSL, 75005 Paris, France

(Received 18 July 2023; revised 23 February 2024; accepted 26 February 2024; published 1 April 2024)

An approximate quantum state preparation method is introduced, called the Walsh series loader (WSL). The WSL approximates quantum states defined by real-value functions of single real variables with a depth independent of the number n of qubits. Two approaches are presented. The first one approximates the target quantum state by a Walsh series truncated at $O(1/\sqrt{\epsilon})$, where ϵ is the precision of the approximation in terms of infidelity. The circuit depth is also $O(1/\sqrt{\epsilon})$, the size is $O(n+1/\sqrt{\epsilon})$, and only one ancilla qubit is needed. The second method accurately represents quantum states with sparse Walsh series. The WSL loads s-sparse Walsh series into n qubits with a depth doubly sparse in s and k, the maximum number of bits with value 1 in the binary decomposition of the Walsh function indices. The associated quantum circuit approximates the sparse Walsh series up to an error ϵ with a depth $O(sk)$, a size $O(n+sk)$, and one ancilla qubit. In both cases, the protocol is a repeat-until-success procedure with a probability of success $P=\Theta(\epsilon)$, giving an averaged total time of $O(1/\epsilon^{3/2})$ for the WSL and $O(sk/\epsilon)$ for the sparse WSL. Amplitude amplification can be used to reach a probability of success $P=\Theta(1)$, modifying the quantum circuit size to $\tilde{O}((n+1/\sqrt{\epsilon})/\sqrt{\epsilon})$ and $\tilde{O}((n+sk)/\sqrt{\epsilon})$ and the depth to $O([\log(n)^3+1/\sqrt{\epsilon}]/\sqrt{\epsilon})$ and $O([\log(n)^3+sk]/\sqrt{\epsilon})$, respectively. Amplitude amplification reduces by a factor $O(1/\sqrt{\epsilon})$ the total time dependence on ϵ but increases the size and depth of the associated quantum circuits, making them linearly dependent on n. These protocols give overall efficient algorithms with no exponential scaling in any parameter. They can be generalized to any complex-value, multivariate, almost-everywhere-differentiable function. The repeat-until-success Walsh series loader is so far the only method that prepares a quantum state with a circuit depth and an averaged total time independent of the number of qubits.

DOI: 10.1103/PhysRevA.109.042401

I. INTRODUCTION

The second quantum revolution relies on the manipulation of individual quantum systems. One of the key technologies promised by this revolution is quantum computing, which is made possible by the manipulation of individual quantum bits (qubits). Because they can use quantum superposition and entanglement, quantum computers (QCs) will perform some computations faster than classical computers and mapping computationally demanding problems into a form tractable by a QC has become an active area of research.

Loading classical data into an n-qubit state is called quantum state preparation (QSP) and is a fundamental subroutine in many prevalent quantum algorithms. For instance, quantum machine learning uses classical training data sets as input [1–3] and the quantum Monte Carlo method uses QSP to achieve a quadratic speedup in reaching hitting time and computing expectation values of functions [4–8]. Also, addressing the electronic structure problem on a quantum computer involves initializing the qubits to a well-chosen state, typically an approximation of the system's ground state [9], Hamiltonian simulation using qubitization has its computational cost estimated in the number of calls to a QSP oracle [10], and solving linear system of equations $Ax=b$ using quantum computers relies on preparing a qubit state $|b\rangle$ encoding the vector b [11,12]. In particular, the problem of solving partial differential equations (PDEs) on QCs has recently attracted a great deal of attention, with publications discussing digital quantum algorithms [13–26], hybrid and variational quantum-classical methods [26–33], and adiabatic and annealing quantum algorithms [34–40]. To solve the Cauchy problems for differential equations on any digital computer, be it classical or quantum, one needs to (i) discretize space and time and (ii) load the initial condition onto the computer. For these different problems, the set of classical data can always be represented by a function f of a certain variable x, where both x and f are possibly multidimensional with some smoothness properties.

Encoding classical data into an n-qubit state may cost an exponential number of primitive operations because the space of all n-qubit states has dimension 2^n. Thus, exact methods for QSP have an exponential scaling with n in size, i.e., the total number of primitive quantum gates, in depth, i.e., the number of layers of primitive quantum gates, or in the number of ancilla qubits [41–47]. It has been suggested that these issues can be overcome by using quantum generative adversarial networks and variational methods with low depth and size trained quantum circuits [48,49]. However, these methods suffer from usual optimization problems such as barren plateaus, local minima, and scalability [50,51]. This has prompted the introduction of new schemes exploiting the structure of the classical data (sparsity, smoothness, etc.) to achieve efficient complexities scaling at most as $O(\text{poly}(n,1/\epsilon))$, avoiding in particular exponential scalings [52–54].

In this article we present a simple quantum algorithm for QSP based on Walsh functions: the Walsh series loader

TABLE I. Scaling laws of the depth, size, probability of success, and averaged total time for the WSL and for the sparse WSL with repeat-until-success and amplitude amplification protocols. The number of qubits is n, the sparsity of the Walsh series is s, and $k \leqslant n$ is the maximum Hamming weight of the indices of the Walsh functions appearing in the sparse Walsh series. For the WSL (sparse WSL), ϵ is the error in terms of infidelity between the implemented state and a target quantum state $|f\rangle$ ($|f_s\rangle$) associated with a differentiable function f (a sparse Walsh series f_s). The notation $\tilde{O}$ is defined as O notation up to a polylogarithmic factor $\log(n)^4$.

Method		Depth	Size	Probability of success	Averaged total time
repeat until success	WSL	$O(1/\sqrt{\epsilon})$	$O(n+1/\sqrt{\epsilon})$	$\Theta(\epsilon)$	$O(1/\epsilon^{3/2})$
repeat until success	sparse WSL	$O(sk)$	$O(n+sk)$	$\Theta(\epsilon)$	$O(sk/\epsilon)$
amplitude amplification	WSL	$O([\log(n)^3+1/\sqrt{\epsilon}]/\sqrt{\epsilon})$	$\tilde{O}((n+1/\sqrt{\epsilon})/\sqrt{\epsilon})$	$\Theta(1)$	$O([\log(n)^3+1/\sqrt{\epsilon}]/\sqrt{\epsilon})$
amplitude amplification	sparse WSL	$O([\log(n)^3+sk]/\sqrt{\epsilon})$	$\tilde{O}((n+sk)/\sqrt{\epsilon})$	$\Theta(1)$	$O([\log(n)^3+sk]/\sqrt{\epsilon})$

(WSL). The set of Walsh functions was first introduced by Walsh [55], who showed that every continuous function of bounded variations defined on [0,1] can be expanded into a series of Walsh functions. Consider, for example, a set of classical data corresponding to a real-value function f of a single real variable. Starting from the Walsh series of f, also called the Walsh-Hadamard series, one can implement a quantum state ϵ-close to the target quantum state using only one ancilla qubit, with a quantum circuit of depth $O(1/\sqrt{\epsilon})$ independent of the number of qubits n and of size $O(n+1/\sqrt{\epsilon})$. The efficiency of the algorithm is guaranteed for any function with a bounded first derivative. The algorithm also applies to complex-value functions and/or functions of d real variables loaded into nd qubits. More generally, the WSL can load any Walsh series of s terms up to an error $\epsilon > 0$ with a quantum circuit of depth $O(sk)$ and size $O(n+sk)$, where k is the maximum number of bits with value 1 in the binary decomposition of the Walsh function indices (maximum Hamming weight of the Walsh function indices). The protocol is presented as a repeat-until-success procedure with a probability of success $P=\Theta(\epsilon)$ and an averaged time for success given by $T = D/P$, where D denotes depth. Amplitude amplification can be performed to increase the probability of success to $P=\Theta(1)$ and decrease the averaged total time by a factor $O(1/\sqrt{\epsilon})$, all at the cost of increasing the quantum circuit size and depth. All complexity scalings are summarized in Table I.

This article is organized as follows. Section II defines Walsh functions, Walsh series, and their associated operators. Section III introduces the Walsh series loader, its features, and complexities. Section IV illustrates the efficiency of the WSL with numerical examples. Section V discusses and compares the WSL with other QSP algorithms for smooth functions. We briefly summarize in Sec. VI.

II. PRELIMINARIES ON WALSH FUNCTIONS AND WALSH OPERATORS

Walsh functions form a set of orthogonal functions defined on [0,1] by

$$w_j(x) = (-1)^{\sum_{i=1}^n j_i x_{i-1}}, \tag{1}$$

where j is the order of the Walsh function, j_i is the ith bit in the binary expansion $j=\sum_{i=1}^n j_i 2^{i-1}$, and x_i is the ith bit in the dyadic expansion $x=\sum_{i=0}^\infty x_i/2^{i+1}$. Walsh functions are ideal in the general context of binary logic and binary arithmetic and in particular in quantum information. Indeed, the operator $\hat{w}_j$ associated with the Walsh function w_j can be written as a tensor product of Pauli Z gates $\hat{w}_j = (Z_1)^{j_1}\otimes\cdots\otimes(Z_n)^{j_n}$, where j_i is the ith coefficient in the binary expansion of $j=\sum_{i=1}^n j_i 2^{i-1}$. Given a function f of the variable $x\in[0,1]$, one can expand it in terms of Walsh functions $f=\sum_{j=0}^\infty a_j w_j$.[1] On a finite set of M points, one can exactly expand the restricted function f as a series of M Walsh functions. On [0,1], the M Walsh series approximate the function f up to an error ϵ_1. More precisely, choosing $M=2^m$ with $m=\lceil\log_2(1/\epsilon_1)\rceil$ gives an error $\|f'\|_\infty\epsilon_1$ between f and its M Walsh series

$$f^{\epsilon_1} = \sum_{j=0}^{M(\epsilon_1)-1} a_j^f w_j \tag{2}$$

such that $\|f-f^{\epsilon_1}\|_\infty \leqslant \|f'\|_\infty\epsilon_1$ (see Lemma 2 in Appendix B). The jth Walsh coefficient a_j^f associated with the function f is defined by

$$a_j^f = \frac{1}{M}\sum_{k=0}^{M-1} f(k/M)w_j(k/M). \tag{3}$$

Walsh series play a crucial role in the efficient implementation of diagonal unitaries on a set of n qubits. Bullock and Markov [56] proved that implementing an exponential of the Walsh operator $\hat{W}_j = e^{a_j\hat{w}_j}$ is optimal by considering the set of Walsh coefficients a_j associated with the phases $\{\theta_j\}$ of a diagonal unitary $e^{i\hat{\theta}} = \sum_j e^{i\theta_j}|j\rangle\langle j|$. Each operator $\hat{W}_j$ is then implemented using two controlled-NOT (CNOT) stairs and one $\widehat{\mathrm{RZ}} = e^{ia_j\hat{Z}}$ gate (more details in Appendix A 1). Then Welsh *et al.* [57] introduced the first efficient quantum circuit for diagonal unitaries based on M Walsh series. The Walsh series loader exploits these constructions and introduces sparse Walsh series to achieve quantum state preparation.

III. WALSH SERIES LOADER

Assume for the time being that f is a real-value function of the single real variable $x\in[0,1]$. The QSP algorithm consists

[1]In other words, Walsh functions can be used to perform harmonic analysis.

in preparing the qubit state

$$|f\rangle = \frac{1}{\|f\|_{2,N}} \sum_{x\in\mathcal{X}_n} f(x)|x\rangle\,, \tag{4}$$

where the kets $|x\rangle$ are eigenstates of the operator representing the classical variable x. Also, $\mathcal{X}_n = \{0, 1/N, \dots, (N-1)/N\}$, $\|f\|_{2,N} = \sqrt{\sum_{j=0}^{N-1} f(j/N)^2}$, and $N = 2^n$, with n the number of qubits.

The quantum algorithm for QSP that we propose is based on two key ingredients. The first one is an efficient implementation of diagonal unitary operators through Walsh operators: Consider, for any given f, the operator $\hat{f} = \sum_{x\in\mathcal{X}_n} f(x)|x\rangle\langle x|$ and the unitary operator $\hat{U}_{f,\epsilon_0} = e^{-i\hat{f}\epsilon_0}$, where ϵ_0 is an arbitrary strictly positive real number. Both operators are diagonal in the x basis. At a given ϵ_0, the operator $\hat{U}_{f,\epsilon_0}$ contains all the information present in the state $\hat{f}$. So encoding $\hat{U}_{f,\epsilon_0}$ in an efficient way is tantamount to encoding the information present in $|f\rangle$ in an efficient way. This is possible by first approximating f with an M Walsh series (or a sparse Walsh series with only a number s of Walsh functions) and then implementing the corresponding exponential of Walsh operators.

The second ingredient in the algorithm is a repeat-until-success method which transforms the unitary $\hat{U}_{f,\epsilon_0} = e^{-i\hat{f}\epsilon_0}$ into an operator proportional to $\hat{f}$ and ultimately into the desired quantum state $|f\rangle$. This is achieved by an interference scheme where an ancilla qubit is manipulated to generate the operator $\hat{I} - e^{-i\hat{f}\epsilon_0}$, which, for small enough ϵ_0, coincides with $i\hat{f}\epsilon_0$. It turns out that measuring the ancilla qubit delivers, at leading order in ϵ_0, the desired state $|f\rangle$. This is so because measurement introduces an extra normalization factor $\mathcal{N} \propto \epsilon_0$ which, at leading order in ϵ_0, cancels the ϵ_0 dependence present in $\hat{I} - e^{-i\hat{f}\epsilon_0}$.

Let us now give some details about the way the ancilla qubit is used. Suppose that the n-qubit register for the position x is initially in the state $|0,\dots,0\rangle$. We apply to the register a Hadamard tower to get from that state the uniform superposition

$$|s\rangle = \hat{H}^{\otimes n}|0,\dots,0\rangle = \frac{1}{\sqrt{N}} \sum_{x\in\mathcal{X}_n} |x\rangle\,, \tag{5}$$

with $N = 2^n$ and n the number of qubits. We then add an ancillary qubit in state $|q_A\rangle = \hat{H}|0\rangle = \frac{1}{\sqrt{2}}(|0\rangle + |1\rangle)$, so the state of the total system is $|\psi_1\rangle = \frac{1}{\sqrt{2}}(|s\rangle|0\rangle + |s\rangle|1\rangle)$. We now let the ancilla control the action of $\hat{U}_{f,\epsilon_0}$ by introducing a new controlled-$\hat{U}_{f,\epsilon_0}$ operator whose action on $|\psi_1\rangle$ gives

$$|\psi_2\rangle = \frac{1}{\sqrt{2}}(|s\rangle|0\rangle + e^{-i\hat{f}\epsilon_0}|s\rangle|1\rangle). \tag{6}$$

Technically, a quantum circuit for controlled–$\hat{U}_{f,\epsilon_0}$ operation can be obtained from a quantum circuit for $\hat{U}_{f,\epsilon_0}$ by letting every gate be controlled by the ancilla qubit, changing CNOT gates into Toffoli gates and single-qubit rotations into controlled rotations. The Hadamard gate $\hat{H}$ and the gate $\hat{P} = \begin{pmatrix}1 & 0\\ 0 & -i\end{pmatrix}$ can then be used to mix components and get the

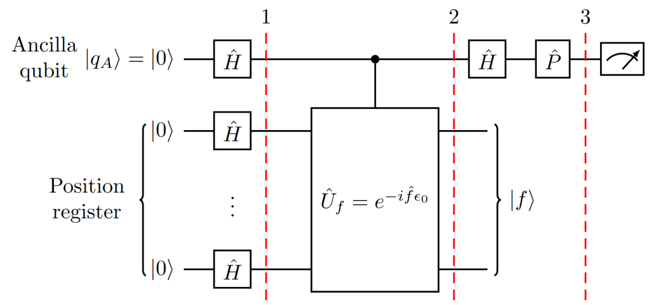

FIG. 1. Quantum circuit for the preparation of an initial quantum state $|f\rangle = \frac{1}{\|f\|_2}\sum_x f(x)|x\rangle$ associated with a real-value function f. At each red dashed line, the quantum state corresponds to Eqs. (5), (2), (3), and (4), respectively.

state

$$|\psi_3\rangle = \frac{\hat{I} + e^{-i\hat{f}\epsilon_0}}{2}|s\rangle|0\rangle - i\frac{\hat{I} - e^{-i\hat{f}\epsilon_0}}{2}|s\rangle|1\rangle\,. \tag{7}$$

We then measure the ancilla qubit (in the computational basis). If $|q_A\rangle = |0\rangle$, the protocol starts again. If $|q_A\rangle = |1\rangle$, the output state is

$$|\psi_4\rangle = -i\frac{\hat{I} - e^{-i\hat{f}\epsilon_0}}{2\|\frac{\hat{I}-e^{-i\hat{f}\epsilon_0}}{2}|s\rangle\|_{2,N}}|s\rangle \simeq |f\rangle + O(\epsilon_0), \tag{8}$$

which, at leading order in ϵ_0, is identical to the desired state. Note that the very act of measuring the ancilla introduces the correct renormalization, which makes it possible to obtain the desired state. The part of the algorithm that we have just described, which involves the ancilla qubit, is represented in Fig. 1.

The probability of success of the protocol, i.e., the probability $P(1)$ to measure $|q_A\rangle = |1\rangle$, scales as

$$P(1) = \left\|\frac{\hat{I} - e^{-i\hat{f}\epsilon_0}}{2}|s\rangle\right\|_{2,N}^2 \simeq \frac{\epsilon_0^2}{4N}\|f\|_{2,N}^2 \simeq \frac{\epsilon_0^2}{4}\|f\|_{2,[0,1]}^2. \tag{9}$$

In the case of interest where f is a continuous function on [0,1], f is also in $L_2([0,1])$, so the quantity $\frac{1}{N}\|f\|_{2,N}^2 = \sum_{j=0}^{N-1} f(j/N)^2/N$ is bounded and tends to $\|f\|_{2,[0,1]}^2 = \int_0^1 f(x)^2 dx$, giving a probability of success asymptotically independent of N. In some other particular cases, for instance, with a Dirac distribution $f(x) = \delta(x - 0.5)$, the probability of success is exponentially small with N, leading to an inefficient method.[2] Note that the probability $P(1)$ is controlled by the L^2-norm of f, not by the derivative f'. The derivative, however, controls how well the Walsh series represent f.

The repeat-until-success procedure does not increase the size or the depth of the quantum circuit. On average, the time T required to achieve success equals the depth of the quantum circuit D divided by the probability of success $T = D/P(1)$. Once success is reached, the QSP has been performed. Furthermore, one could perform amplitude amplification to reach

[2]For sparse functions defined as the sum of Dirac functions, efficient QSP exists [9].

$P(1) = \Theta(1)$. Amplitude amplification reduces quadratically the total time T with respect to the number of trials in the repeat-until-success procedure, i.e., $T = D'/\sqrt{P(1)}$, with D' the depth of the quantum circuit performing one reflection of the amplitude amplification (more details in Appendix C). Therefore, the total time is reduced by a factor $1/\epsilon_0$ (or $1/\sqrt{\epsilon}$ in Table I) but at the cost of increasing the size and the depth of the WSL, making them dependent of n with a polylogarithmic factor. This quadratic improvement with respect to $P(1)$ is similar to the quadratic advantage of the Grover algorithm.

This procedures works for real-value functions f, but it obviously fails if f is complex valued, because a complex-value f makes the operator $\hat{U}_{f,\epsilon_0}$ nonunitary. The way to handle complex-value functions is to add a layer to the algorithm. One introduces the modulus $|f|$ and the phase ϕ_f. One carries out the above procedure for $|f|$ (instead of f) and then implements efficiently the unitary operator $\exp(i\phi_f)$ separately using again Walsh functions as developed in [57], adding an additional $O(1/\sqrt{\epsilon})$ in terms of size and depth (more details in Appendix A 2).

Error analysis. The discrepancy between the target quantum state and the implemented quantum state has two distinct origins. The first one is the error ϵ_1 introduced by computing the finite Walsh series of f on a set of $M(\epsilon_1)$ points. The second one is the error ϵ_0 introduced by the interference scheme.

Let us be a bit more specific about the first source of error. The diagonal unitary operator $\hat{U}_f$ is implemented efficiently using the scheme introduced by Welsh *et al.* in [57]. The differentiable real function f defined on [0,1] is expanded into a Walsh series f^{ϵ_1}. The Walsh series of f corresponds to a piecewise constant function which coincides with f on a finite number of points and the error associated with the Walsh series can be bounded by the maximum value of the first derivative of f on [0,1]: $\|f(x) - f^{\epsilon_1}(x)\|_\infty \leqslant \epsilon_1 \|f'\|_\infty$, where $\|f\|_\infty = \sup_{x\in[0,1]} |f(x)|$. These two errors result in an infidelity $1 - F = O((\epsilon_0 + \epsilon_1\|f'\|_\infty)^2)$, emphasizing the fact that the method is efficient for slowly varying functions, i.e., when the space step of the discretization of the continuous problem is small compared to the characteristic length of variations of the PDE problem.

The results of this article can be summarized in two theorems. First, consider a state defined by a real-value function f defined on $[0, 1]^d$ and suppose one wants to load that state to $n = \sum_{i=1}^d n_i$ qubits with errors $\vec{\epsilon} = (\epsilon_1, \dots, \epsilon_d)$. Then we have the following theorem.

Theorem 1. There is an efficient quantum circuit of size $O(n_1 + \dots + n_d + 1/(\epsilon_1 \times \dots \times \epsilon_d))$ and depth $O(1/(\epsilon_1 \times \dots \times \epsilon_d))$, which, using one ancillary qubit, implements the quantum state $|f\rangle$ with a probability of success $P(1) = \Theta(\epsilon_0^2)$ and infidelity $1 - F = O((\epsilon_0 + \sum_{i=1}^d \epsilon_i \|\partial_i f\|_{\infty,[0,1]^d})^2)$.

The proof of this theorem can be found in Appendix B. If one wants to quantify the infidelity by a single small parameter $\epsilon > 0$, one can choose $\epsilon_0 \propto \sqrt{\epsilon}$ and $\epsilon_1 \propto \sqrt{\epsilon}$. In the particular one-dimensional case, Theorem 1 ensures that there is a quantum circuit of size $O(n + 1/\sqrt{\epsilon})$ and depth $O(1/\sqrt{\epsilon})$, which uses only one ancillary qubit and implements the quantum state $|f\rangle$ with a probability of success $P(1) = \Theta(\epsilon)$ and infidelity $1 - F \leqslant \epsilon$. Also, note that the size is affine in $n_1 + \dots + n_d$ (or n) because of the Hadamard gates applied on each qubit at the first step of the QSP algorithm.

Additionally, real-value functions which are accurately represented by a sparse Walsh series of s terms can be efficiently loaded to n qubits. Let us consider $f \simeq f_s := \sum_{j\in S} a_j w_j$ with $S \subset \{0, 1, \dots, 2^n - 1\}$, where the a_j's can be chosen to minimize the difference between f_s and f. The problem of finding the best set S and the best coefficients $\{a_j, j \in S\}$ to approximate a function f is called the minimax series problem [58]. A simple but efficient way to find a sparse Walsh series approximating a given function f is to keep in the Walsh series of f the terms with the largest $|a_j|$. The complexity of implementing a given s-sparse Walsh series depends directly on s and k, the maximum Hamming weight of the binary decomposition of the Walsh coefficient indices: $k = \max_{j\in S}(\sum_{i=0}^{l_j} j_i)$, with $j = \sum_{i=0}^{l_j} j_i 2^i$.

Theorem 2. For a given set $S \subset \{0, 1, \dots, 2^n - 1\}$ and real Walsh coefficients $\{a_j, j \in S\}$ there is an efficient quantum circuit of size $O(n + sk)$ and depth $O(sk)$ which, using one ancillary qubit, implements the quantum state $|f_s\rangle$ with a probability of success $P(1) = \Theta(\epsilon)$ and infidelity $1 - F \leqslant \epsilon$.

A corollary of Theorem 2 concerns the case of a function f approximated by a sparse Walsh series f_s such that $\|f - f_s\|_\infty \leqslant \sqrt{\epsilon}$. Then there is an efficient quantum circuit of size $O(n + sk)$ and depth $O(sk)$ which, using one ancillary qubit, implements the quantum state $|f\rangle$ with a probability of success $P(1) = \Theta(\epsilon)$ and infidelity $1 - F \leqslant \epsilon$. On n qubits, the parameter k is necessarily smaller than or equal to n. So in the worst-case scenario the sparse WSL method has depth $O(sn)$ and size $O(sn)$. The proof of this theorem and corollary can be found in Appendix B.

IV. NUMERICAL RESULTS

The scaling laws stated in Theorem 1 can be illustrated by numerical examples. Figure 2 displays, for various functions, how the infidelity $1 - F$ scales with $\epsilon = \epsilon_0^2 = \epsilon_1^2$ [Fig. 2(a)] and with n [Fig. 2(b)]. Figure 2(a) confirms the linear scaling with ϵ while Fig. 2(b) clearly illustrates the fact that, for a given target state, the infidelity admits an n-independent (but ϵ-dependent) upper bound. Note that the optimal infidelity is given for $M = N$ and $\epsilon_0 = \epsilon_1 = 1/N$, but this case needs an exponential amount of resources to be implemented.

Furthermore, the WSL offers two ways of arranging the Walsh operators. The first one is to use a Gray code which cancels a maximum number of CNOT gates: Out of two CNOT stairs, only one CNOT remains, reaching optimality in terms of size [56,57]. The second method consists in implementing a sparse Walsh series by listing the M Walsh coefficients of f in decreasing order, keeping then only the first, dominant coefficients. One can thus obtain surprisingly accurate approximations of the targeted state with a very small number of Walsh operators. Numerical results show that, at a given infidelity, the second method has a depth smaller than the first method (see Fig. 3). The dominant Walsh coefficients actually do not depend on the total number of qubits n. The procedure thus delivers another QSP method with depth independent of n. The number of classical computations needed to implement the Gray code or the decreasing order method depends only

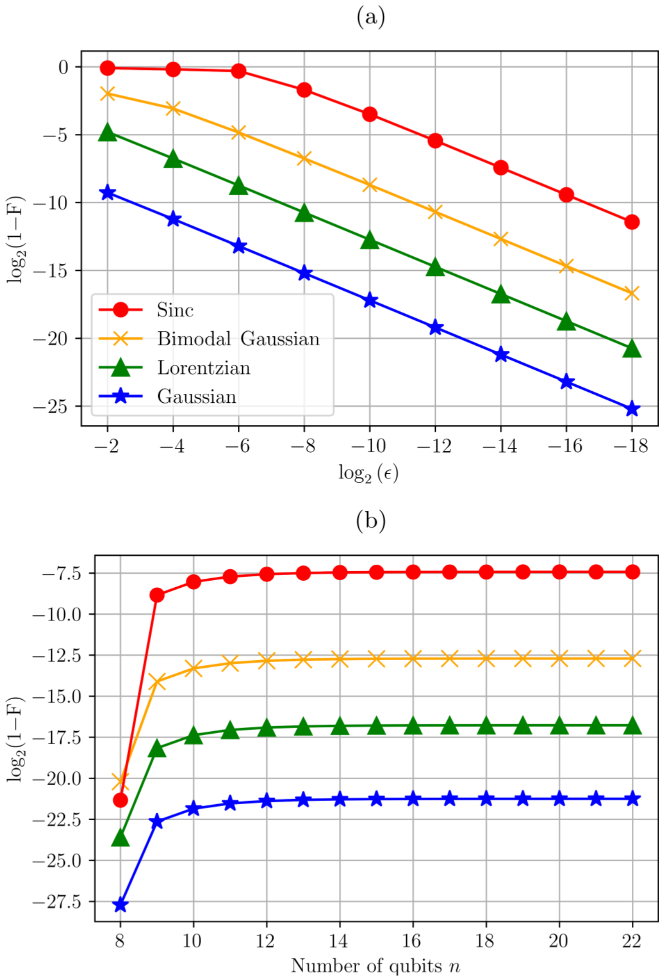

FIG. 2. Infidelity $1-F$ (a) as a function of ϵ with $\epsilon_0=\sqrt{\epsilon}$ and $\epsilon_1=\sqrt{\epsilon}$ for $n=20$ qubits and (b) as a function of n for $\epsilon_0=\epsilon_1=1/2^7$ for different probability distributions: Gaussian $g_{\mu,\sigma}(x)=\exp[-(x-\mu)^2/2\sigma^2]/\sigma$ with $\mu=0.5$ and $\sigma=1$; bimodal Gaussian $g_{\mu_1,\sigma_1,\mu_2,\sigma_2,s}(x)=sg_{\mu_1,\sigma_1}(x)+(1-s)g_{\mu_2,\sigma_2}(x)$ with $\mu_1=0.25$, $\mu_2=0.75$, $\sigma_1=0.3$, $\sigma_2=0.04$, and $s=0.1$; Lorentzian $L_{\mu,\Gamma}(x)=[\Gamma+4(x-\mu)^2/\Gamma]^{-1}$ with $\mu=0.5$ and $\Gamma=1$; and $\text{sinc}(x)=\sin(6\pi x)/6\pi x$.

on M and not n. More details on the WSL for complex and nondifferentiable functions can be found in Appendix A.

V. DISCUSSION AND COMPARISON WITH OTHER METHODS

Our method needs $n+1$ Hadamard gates to initialize the state into a full superposition of all possible ket vectors. The control diagonal unitary which is applied afterward can be implemented with M controlled-Z rotations ($\widehat{\text{CRZ}}$) and $M-1$ Toffoli gates, where M depends on ϵ_1, which is the error made in representing the function f by its Walsh series f^{ϵ_1}. To be precise, $M=2^m$ with $m=\lfloor\log_2(1/\epsilon_1)\rfloor+1$. Now each Toffoli gate can be decomposed into six CNOT gates, two Hadamard gates, and seven $\hat{T}$ and $\hat{T}^\dagger$ gates, without using ancilla qubits [59], and each two-qubit gate $\widehat{\text{CRZ}}(\theta)$ can be decomposed into two CNOT gates and three $\widehat{\text{RZ}}$ gates with the formula $\widehat{\text{CRZ}}(\theta)=[\hat{I}_2\otimes\widehat{\text{RZ}}(\theta)]\text{CNOT}[\hat{I}_2\otimes\widehat{\text{RZ}}(-\theta/2)]\text{CNOT}[\hat{I}_2\otimes\widehat{\text{RZ}}(-\theta/2)]$ [60]. Finally, a Hadamard gate and an optional phase gate $\hat{P}=\begin{pmatrix}1&0\\0&-i\end{pmatrix}=\hat{S}\hat{Z}$, with $\hat{S}=\begin{pmatrix}1&0\\0&i\end{pmatrix}$, are performed on the ancilla qubit, giving a total count of $8M-6$ CNOT gates, $n+2M$ Hadamard gates, $3M$ $\widehat{\text{RZ}}$ gates, $7M-7$ $\hat{T}$ and $\hat{T}^\dagger$ gates, and optional $\hat{Z}$ and $\hat{S}$ gates. This leads to a size scaling as $O(n+1/\epsilon_1)$ and a depth $O(1/\epsilon_1)$. Note that the complexity scalings are given as a function of ϵ_1 because ϵ_1 is linked to the target error, which is an input parameter of the problem, while M is not an input parameter of the problem. Nevertheless, the scalings with m or M are equivalent to the one stated here.

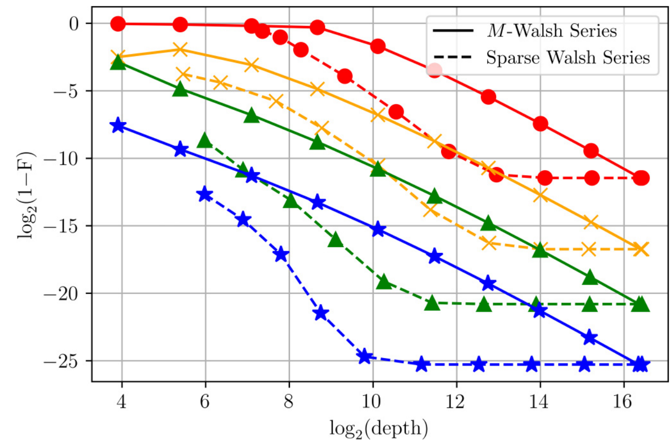

FIG. 3. Infidelity $1-F$ as a function of the depth of the quantum circuits associated with the Gray code order (solid lines) and the decreasing order (dashed lines) for the functions defined in Fig. 2 and the parameters $n=16$ and $\epsilon_0=10^{-3}$. Each symbol corresponds to a number of Walsh operators 2^m going from 2^1 to 2^{10}. For the Gray code order, the 2^m Walsh series is computed for each point. For the decreasing order method, 2^{10} Walsh coefficients are computed and only the 2^m largest are implemented.

In the case of loading an s-sparse Walsh series of the parameter k, the controlled-$\hat{W}_{j,\epsilon_0}$ operator is implementable for each of the s Walsh operators with a quantum circuit composed of two Toffoli stairs of $H(j)$ Toffoli gates, with $H(j)$ the Hamming weight of the binary decomposition of j such that $k=\max_{j\in S}H(j)\leqslant n$, and one $\widehat{\text{CRZ}}$ rotation. The number of Toffoli gates is bounded by $2ks$ and the number of $\widehat{\text{CRZ}}$ is s. In the worst-case scenario, this gives a total of $12k+2s$ CNOT gates, $4ks+n+2$ Hadamard gates, $14ks$ $\hat{T}$ and $\hat{T}^\dagger$ gates, $3s$ $\widehat{\text{RZ}}$ gates, and optional $\hat{S}$ and $\hat{Z}$ gates. In many particular cases, the number of Toffoli gates can be reduced by choosing the order of implementation of the Walsh operators which cancel a maximum number of Toffoli gates in two successive Toffoli stairs. Several algorithms minimize the number of gates in a quantum circuit composed only of CNOT, Toffoli, and RZ gates using phase polynomial synthesis for fully connected hardware and hardware with constrained connectivity [61]. As expected, the Gray code ordering appears as the optimal solution in the case of a dense Walsh series with $s=2^m$ and $k=m$ and it reduces the gate complexity up to a factor $2m$. These results can be compared to other approximate QSP algorithms preparing quantum states associated with continuous functions.

The recent Fourier series loader [53] makes it possible to prepare continuous functions with a depth linear in the number of Fourier components and in the number of qubits. The idea behind this method is to first load the 2^m Fourier components of the target f on the quantum computer and then apply an inverse quantum Fourier transform to get the function f in real space. This result can be compared to ours since the number of Fourier components in the Fourier series of a function can be directly related to the error one makes in the truncation, leading to a gate complexity scaling at most as $O(1/\epsilon^{1/p})$ for p-differentiable functions. Nevertheless, the inverse QFT leads to a final quantum circuit of size $O(n^2 + 2^m)$ and depth $O(n + 2^m)$, while the Walsh series loader has only size $O(n + 2^m)$ and depth $O(2^m)$ [and a probability of success $P(1) = \Theta(\epsilon_0^2)$]. This difference mainly comes from the fact that Walsh series can be loaded directly in real space.

In [54], quantum state preparation for continuous real functions f_1 is achieved going adiabatically from the Hamiltonian $H_0 = |f\rangle\langle f|$, with $|f\rangle = H^{\otimes n}|0\rangle$, to the target Hamiltonian $H_1 = |f_1\rangle\langle f_1|$. The adiabatic evolution is implemented via small Trotterization steps. To thus prepare the target quantum state with error ϵ, the query complexity is $O(\mathcal{F}^p/\epsilon^2)$, where $\mathcal{F}$ is a constant depending on f_1, and the number of necessary ancilla qubits scales as $O(n + d)$, where d is the number of digits used in the discretized encoding of f_1. Even if the WSL is a repeat-until-success procedure, it offers a quadratic advantage in terms of size and depth due to the fact that the complexity scales with the $L2$ error ϵ ($\frac{1}{\epsilon}$ instead of $\frac{1}{\epsilon^2}$) and necessitates only one ancilla qubit.

Another method [62] suggests the approximation of quantum states associated with smooth, differentiable, and real-value (SDR) functions using matrix product state (MPS) methods. Approximating SDR functions as polynomials admitting the MPS representation, one can use MPS compressions and mappings from MPS representations to quantum circuits. The presented quantum circuits are linear in n (depth and size) and are obtained with a linear number of classical computations. However, Ref. [62] offers only empirical arguments in favor of the method's efficiency and does not produce analytically proven scaling laws involving the error ϵ.

Another approximate QSP method [52] makes use of a modified version of the Grover-Rudolph algorithm [41]. To load a real-value, positive, and twice-differentiable function on n qubits with infidelity less than ϵ, Marin-Sanchez *et al.* implement only $2^{k(\epsilon,n)} - 1$ multicontrolled rotations (instead of 2^n) with $k(\epsilon, n)$ asymptotically independent of n. For other functions, Marin-Sanchez *et al.* use a variational generalization of the original algorithm. Even if the Walsh series loader presented above is a repeat-until-success procedure, it does not involve variational steps and it can be used for any once- (as opposed to twice-) differentiable functions, including real-value but nonpositive functions, complex functions, or even multivariate ones. Also, the depth of the WSL is not only asymptotically but exactly independent of the number of qubits n.

VI. CONCLUSION

The WSL algorithms approximate quantum states efficiently with a depth independent of the number of qubits. This remarkable property brings us one step closer to quantum supremacy for all algorithms needing a QSP step. This work should be extended by investigating other alternative methods to compute finite Walsh series approximations. Possible candidates include threshold sampling, data compression [58], or efficient estimation of the number M of best Walsh coefficients [63].

ACKNOWLEDGMENTS

The authors thank N. F. Loureiro, A. B. Grilo, T. Fredon, U. Remond, and U. Nzongani for useful feedback on our research. The quantum circuit diagrams in this paper were prepared using QUANTIKZ package [64] and the plots were prepared using the MATPLOTLIB library [65].

APPENDIX A: TECHNICAL DETAILS ABOUT THE IMPLEMENTATION OF THE WALSH SERIES LOADER

1. Loading of real-value functions

Following the scheme of Welsh *et al.* [57], loading a real-value function f defined on [0,1] to an n-qubit state starts with the discretization of the interval [0,1] into $N = 2^n$ discrete points $\mathcal{X}_n = \{0, 1/N, 2/N, 3/N, \dots, (N-1)/N\}$. The second step consists in computing classically the Walsh coefficients of the function f. The Walsh function of order $j \in \{0, 1, \dots, N-1\}$ is defined by

$$w_j(x) = (-1)^{\sum_{i=1}^{n} j_i x_{i-1}}, \tag{A1}$$

where j_i is the ith bit in the binary expansion $j = \sum_{i=1}^{n} j_i 2^{i-1}$ and x_i is the ith bit in the dyadic expansion $x = \sum_{i=0}^{\infty} x_i/2^{i+1}$.

The M Walsh series f^{ϵ_1} approximating a function f up to an error ϵ_1 is

$$f^{\epsilon_1} = \sum_{j=0}^{M(\epsilon_1)-1} a_j^f w_j, \tag{A2}$$

where $m(\epsilon_1) = \lfloor \log_2(1/\epsilon_1) \rfloor + 1$ and $M(\epsilon_1) = 2^{m(\epsilon_1)}$ with $\frac{1}{M(\epsilon_1)} < \epsilon_1$. The jth Walsh coefficient a_j^f associated with the function f is defined by

$$a_j^f = \frac{1}{M} \sum_{x \in \mathcal{X}_m}^{M-1} f(x) w_j(x), \tag{A3}$$

where $\mathcal{X}_m = \{0, 1/M, 2/M, 3/M, \dots, (M-1)/M\}$.

The last step consists in performing the WSL quantum circuit by implementing the controlled diagonal unitary $\hat{U}_{f^{\epsilon_1},\epsilon_0}$ associated with the computed a_j^f coefficients. Note that the decomposition into one-qubit gates and two-qubit gates of the controlled-$\hat{U}_{f,\epsilon_0}$ operator is given by controlling all the gates coming from the decomposition of $\hat{U}_{f,\epsilon_0}$. Thus, in the

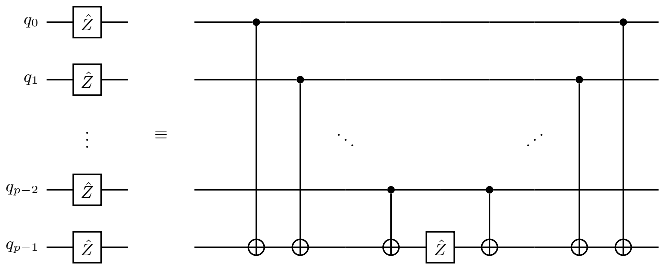

FIG. 4. Equivalent quantum circuit for a tower of p Pauli Z quantum gates.

following we focus only on the decomposition of $\hat{U}_{f^{\epsilon_1},\epsilon_0}$,

$$\hat{U}_{f^{\epsilon_1},\epsilon_0} = e^{-i\hat{f}^{\epsilon_1}\epsilon_0} = \exp\left(-i\sum_{j=0}^{M-1} a_j^f \hat{w}_j \epsilon_0\right) = \prod_{j=0}^{M-1} e^{-ia_j^f \hat{w}_j \epsilon_0} = \prod_{j=0}^{M-1} \hat{W}_{j,\epsilon_0}, \tag{A4}$$

where $\hat{W}_{j,\epsilon_0} = e^{-ia_j^f \hat{w}_j \epsilon_0}$ and the Walsh operators are defined as $\hat{w}_j = (Z_1)^{j_1} \otimes \cdots \otimes (Z_n)^{j_n}$, where j_i is the ith coefficient in the binary expansion of $j = \sum_{i=1}^n j_i 2^{i-1}$. Using the fact that a tensor product of Pauli Z gates can be rewritten using CNOT staircases as (see Fig. 4)

$$\hat{Z}_0 \otimes \cdots \otimes \hat{Z}_{p-1} = \hat{A}_p(\hat{I}_{0:p-2} \otimes \hat{Z}_{p-1})\hat{A}_p^{-1}, \tag{A5}$$

where $\hat{Z}_i$ is the Pauli Z gate acting on qubit i, $\hat{I}_{0:p-2}$ is the identity operator acting on qubits $0, \dots, p-2$, and $\hat{A}_p = \widehat{\mathrm{CNOT}}_0^{p-1} \widehat{\mathrm{CNOT}}_1^{p-1} \cdots \widehat{\mathrm{CNOT}}_{p-2}^{p-1}$, with $\widehat{\mathrm{CNOT}}_i^j$ the CNOT quantum gate controlled by qubit i and applied on qubit j. Therefore, the operator $\hat{W}_{j,\epsilon_0}$ acting on p qubits can be simply written in term of quantum gates as (see Fig. 5)

$$\hat{W}_{j,\epsilon_0} = \hat{A}_p\big(\hat{I}_{0:p-2} \otimes e^{-ia_j^f \epsilon_0 \hat{Z}}\big)\hat{A}_p^{-1}. \tag{A6}$$

Then the $\hat{W}_{j,\epsilon_0}$ commute with each other, allowing us to optimize the order of implementation of the $\hat{W}_{j,\epsilon_0}$. The first method consists in canceling a maximum number of CNOT gates coming from the operators $\hat{A}_q$ of two consecutive $\hat{W}_{j,\epsilon_0}$ and $\hat{W}_{j',\epsilon_0}$. This is done using a Gray code [66]: Only one bit changes in the binary decomposition of the indices j and j' of two consecutive operators. The second method consists in

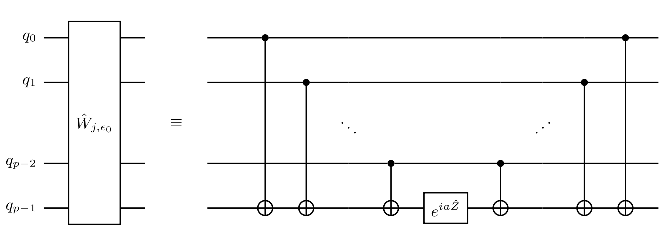

FIG. 5. Quantum circuit for the operator $\hat{W}_j(a)$ acting on p different qubits using CNOT and RZ quantum gates.

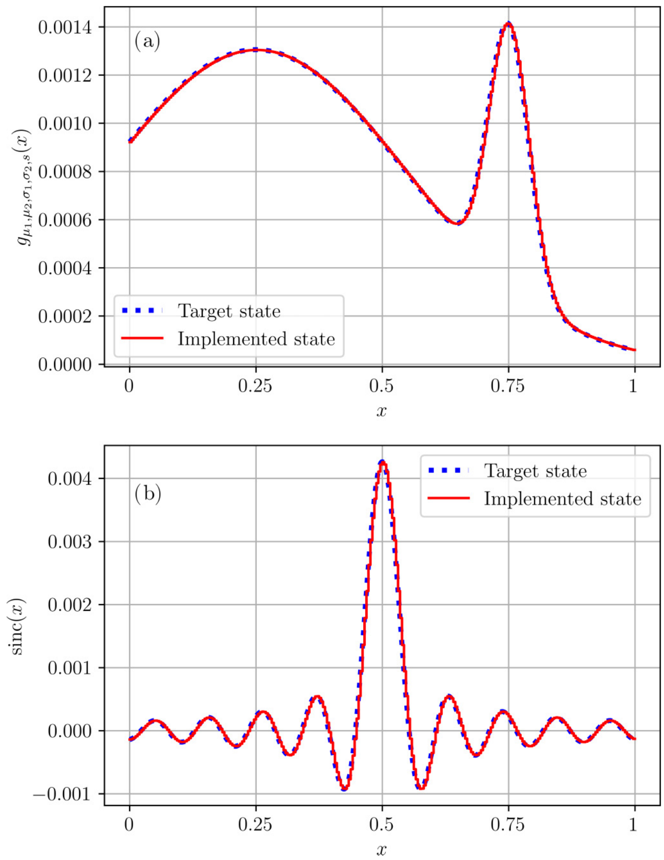

FIG. 6. (a) Quantum state preparation on $n = 20$ qubits of a bimodal Gaussian $g_{\mu_1,\sigma_1,\mu_2,\sigma_2,s}(x) = (1-s)g_{\mu_1,\sigma_1}(x) + sg_{\mu_2,\sigma_2}(x)$, with $g_{\mu,\sigma}(x) = \exp[-(x-\mu)^2/2\sigma^2]/\sigma$, $\mu_1 = 0.25$, $\mu_2 = 0.75$, $\sigma_1 = 0.3$, $\sigma_2 = 0.04$, and $s = 0.1$ with infidelity $1 - F = 1.5 \times 10^{-4}$ using the parameters $\epsilon_0 = 0.01$ and $\epsilon_1 = 1/2^7$ and (b) quantum state preparation of $\mathrm{sinc}(x) = \sin(6\pi x)/6\pi x$ with infidelity $1 - F = 6.0 \times 10^{-3}$ using the parameters $\epsilon_0 = 0.1$ and $\epsilon_1 = 1/2^7$.

sorting the M Walsh coefficients a_j^f in order to implement only a finite number $M' < M$ of operators $\hat{W}_{j,\epsilon_0}$ associated with the largest $|a_j^f|$. The two methods are compared not in terms of infidelity scaling with the number of Walsh operators but in terms of infidelity scaling with the depth of the associated quantum circuits (Fig. 3). While the first method has theoretical guarantees, the second one seems numerically more efficient since it does not implement all the smallest coefficients of the M Walsh series of f. Other methods exist to compute finite Walsh series approximating a given function f using threshold sampling, data compression [58], or efficient estimation of a number M' of the best Walsh coefficients [63], which could be used for quantum state preparation.

Figure 6 illustrates the Gray ordered WSL method on a bimodal Gaussian function and a sinc function on $n = 20$ qubits, with fidelity larger than 0.999 and 0.99, respectively.

2. Loading of complex-value functions

Complex-value functions are especially useful in contexts involving wave propagation. Associated PDEs include the Maxwell equations and the Klein-Gordon, the Dirac, and the Schrödinger equations. Note that complex-value functions

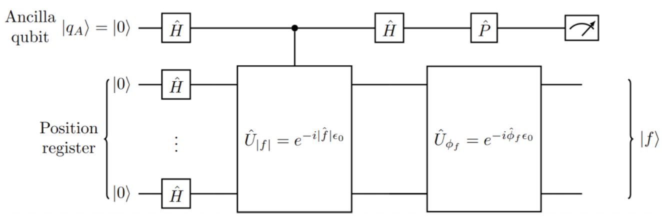

FIG. 7. Quantum circuit for the preparation of an initial quantum state $|f\rangle = \frac{1}{\|f\|_{2,N}} \sum_{x\in\mathcal{X}_n} f(x)|x\rangle$ associated with a complex-value function $f = |f|e^{i\phi_f}$.

are also useful in studying hydrodynamical potential flows [26,67]. The WSL is an efficient method to load the complex-value initial condition for PDEs. Loading of a complex-value function f defined in [0,1] is carried out by first loading the modulus $|f|$ of f and then loading the phase ϕ_f of f. The modulus is loaded with the scheme presented in Fig. 1. The phase ϕ_f is implemented as a diagonal unitary through a Walsh series of ϕ_f using the scheme proposed by Welch *et al.* [57]. The resulting quantum circuit is illustrated Fig. 7. In terms of accuracy, the error one makes in the implementation of f is bounded by the sum of errors one makes in the implementation of $|f|$ and $e^{i\hat{\phi}_f}$.

3. Loading of non-differentiable functions

Applying the WSL on nondifferentiable functions is possible with significant results even if no theoretical guarantees have been proven. In the particular case of real-value functions defined on [0,1] and differentiable almost everywhere but on a finite set of points with a bounded first derivative, Theorem 1 generalizes using the fact that in the proof of Lemma 2 the difference between the function and its Walsh series can be bounded by the maximum of $|f'|$ on each interval where f' is well defined. The WSL is performed for the real-value functions defined on [0,1],

$$
\begin{aligned}
f_1(x) &= \sin[2\pi(x - \tfrac{1}{3})]w_4(x),\\
f_2(x) &= |x - 0.25| - |x - 0.5| + |x - 0.75|,\\
f_3(x) &= \sqrt{|x - 0.5|},\\
f_4(x) &= \frac{1}{1 - x},
\end{aligned}
\tag{A7}
$$

where w_4 is the Walsh function of order 4.

Numerical results in Fig. 8 show scaling laws $1 - F \propto \epsilon$ for continuous nondifferentiable functions such as f_2 and also for noncontinuous functions such as f_1. The scalings are similar to the ones of differentiable functions in Fig. 3. The case of f_3 is particularly interesting since its first derivative is unbounded but the WSL method still provides an accurate QSP method. It could be explained by the fact that f_3 itself is bounded, suggesting that the WSL could converge also for some bounded functions almost everywhere differentiable with an unbounded first derivative. However, in the particular case of a diverging function with a singularity point such as f_4, the WSL fails to accurately prepare the target state due to the diverging values taken by the function in the neighborhood of the singularity. The quantum state preparation of f_1 is presented in Fig. 9 with fidelity larger than 0.99.

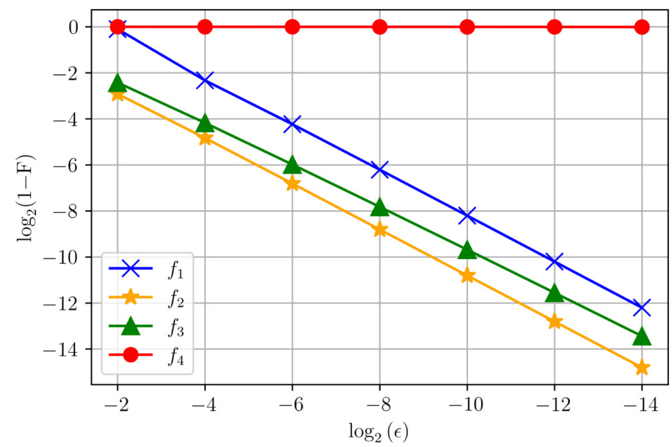

FIG. 8. Scaling laws of the infidelity $1 - F$ with $\epsilon = \epsilon_0^2 = \epsilon_1^2$ for $n = 20$ qubits for some nondifferentiable functions f_1, f_2, f_3, and f_4 defined in Eq. (A7).

APPENDIX B: THEOREMS AND PROOFS

In this Appendix the theorems are stated and proven for the one-dimensional case (Appendixes B 1–B 3), the multi-dimensional case (Appendixes B 4–B 6), and the sparse case (Appendix B 7).

1. Definitions: One-dimensional case

In the following, working on n qubits with an M Walsh series defined on M points associated with a continuous function f defined on [0,1], we must take into account the discrete space $\mathcal{X}_n = \{0, 1/N, \dots, (N-1)/N\}$, with $N = 2^n$, and the continuous space [0,1] with the following norms. For any vector $|\psi\rangle = \sum_{x\in\mathcal{X}_n} \psi(x)|x\rangle \in \mathcal{H}_2^{\otimes n}$,

$$\||\psi\rangle\|_{2,N} = \sqrt{\sum_{x\in\mathcal{X}_n} |\psi(x)|^2}, \tag{B1}$$

$$\||\psi\rangle\|_{\infty,N} = \max_{x\in\mathcal{X}_n} |\psi(x)|. \tag{B2}$$

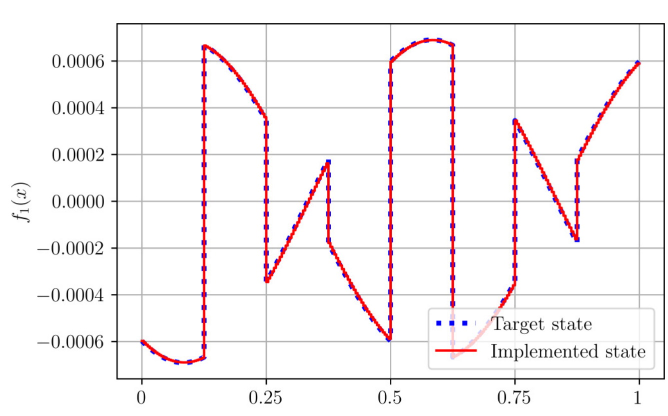

FIG. 9. Quantum state preparation of the nondifferentiable function f_1 defined in Eq. (A7) on $n = 22$ qubits with infidelity $1 - F = 2.1 \times 10^{-3}$ with the parameters $\epsilon_0 = 0.1$ and $\epsilon_1 = 1/2^7$.

For $m < n$ and $M = 2^m$,

$$\| |\psi\rangle \|_{2,M} = \sqrt{\sum_{x\in\mathcal{X}_m} |\psi(x)|^2}. \tag{B3}$$

The fidelity between two states $|\psi_1\rangle \in \mathcal{H}_2^{\otimes n}$ and $|\psi_2\rangle \in \mathcal{H}_2^{\otimes n}$ is

$$F = |\langle\psi_1|\psi_2\rangle|^2 = \left|\sum_{x\in\mathcal{X}_n} \psi_1^*(x)\psi_2(x)\right|^2 \tag{B4}$$

and the infidelity is defined as $1 - F$. For any function f defined on [0,1],

$$\|f\|_{\infty,[0,1]} = \max_{x\in[0,1]} |f(x)|, \tag{B5}$$

$$\|f\|_{\infty,N} = \max_{x\in\mathcal{X}_n} |f(x)|, \tag{B6}$$

$$\|f\|_{2,N} = \sqrt{\sum_{x\in\mathcal{X}_n} |f(x)|^2}, \tag{B7}$$

$$\|f\|_{2,[0,1]} = \sqrt{\int_0^1 |f(x)|^2 dx}. \tag{B8}$$

We note the following properties:

$$\| |\psi\rangle \|_{\infty,N} \leqslant \| |\psi\rangle \|_{2,N} \leqslant \sqrt{N} \| |\psi\rangle \|_{\infty,N}, \tag{B9}$$

$$\|f\|_{\infty,N} \leqslant \|f\|_{2,N} \leqslant \sqrt{N}\|f\|_{\infty,N}, \tag{B10}$$

$$\|f\|_{\infty,N} \leqslant \|f\|_{\infty,[0,1]}, \tag{B11}$$

$$\frac{1}{\sqrt{N}}\|f\|_{2,N} \xrightarrow{N\to+\infty} \|f\|_{2,[0,1]} \,\forall\, f \in \mathcal{C}_0([0,1]), \tag{B12}$$

$$\| |\psi_1\rangle - |\psi_2\rangle \|_{2,N} \leqslant \epsilon \Rightarrow 1 - F \leqslant \epsilon^2. \tag{B13}$$

2. Theorems: One-dimensional case

Let us consider n qubits, a differentiable function f defined on [0,1] such that $\|f\|_{\infty,[0,1]} \neq 0$, $\epsilon_0 \in]0, \pi/\|f\|_{\infty,[0,1]}]$, and $\epsilon_1 > 0$ such that $\|f^{\epsilon_1}\|_{\infty,[0,1]} \neq 0$, where f^{ϵ_1} is the Walsh series of f defined in Eq. (A2).

Theorem 3. There is an efficient quantum circuit of size $O(n + 1/\epsilon_1)$ and depth $O(1/\epsilon_1)$, using one ancillary qubit, to implement a quantum state approximating the target state $|f\rangle$ up to an infidelity $1 - F = O((\epsilon_0 + \epsilon_1\|f'\|_\infty)^2)$ and with a probability of success $P(1) = \Theta(\epsilon_0^2)$.

In the particular case of $\epsilon_1 = \epsilon_0$, we can show the following.

Corollary 1. There is an efficient quantum circuit of size $O(n + 1/\sqrt{\epsilon})$ and depth $O(1/\sqrt{\epsilon})$, using one ancillary qubit, to implement a quantum state approximating the target state $|f\rangle$ up to an infidelity $1 - F \leqslant \epsilon$ with a probability of success $P(1) = \Theta(\epsilon)$.

For any function f with values $f(x)$ calculable in time T_f, the number of classical computations needed to find the quantum circuit is $O(T_f/\epsilon_1^2)$ (Theorem 3) or $O(T_f/\epsilon)$ (Corollary 1).

3. Proofs: One-dimensional case

The proof is based on the six following lemmas.

a. Lemmas

Lemma 1. For any function f continuously defined on [0,1] such that $\|f\|_{\infty,[0,1]} \neq 0$, there exists an n_0 such that for all $n \geqslant n_0$ and for all $\epsilon_0 \in]0, \frac{2\pi}{\|f\|_{\infty,[0,1]}}[$, $\|\frac{\hat{I}-e^{-i\hat{f}\epsilon_0}}{2}|s\rangle\|_{2,N} \neq 0$ with $N = 2^n$.

Proof. First, $\|f\|_{\infty,[0,1]} \neq 0$ implies that there exists an $x_0 \in [0,1]$ such that $f(x) = \|f\|_{\infty,[0,1]} \neq 0$. The continuity of f implies that there exists a neighborhood V of x_0 such that for all $x \in V$, $f(x) \neq 0$. We note the following equality:

$$\left\|\frac{\hat{I} - e^{-i\hat{f}\epsilon_0}}{2}|s\rangle\right\|_{2,N} = \sqrt{\sum_{x\in\mathcal{X}_n} \frac{\sin^2[f(x)\epsilon_0/2]}{N}}. \tag{B14}$$

The ensemble $\mathcal{X}_n = \{0, \frac{1}{N}, \dots, \frac{N-1}{N}\}$, with $N = 2^n$, is a set of dyadic rationals, i.e., numbers with a denominator that can be expressed as a power of 2. Using the fact that dyadic numbers restricted to [0,1] are dense in [0,1], there exist two integers p and q such that $p < 2^q$ and $p/2^q \in V$. Furthermore, $p/2^q \in \mathcal{X}_q = \{0, \dots, \frac{2^q-1}{2^q}\}$ and $p/2^q \in \mathcal{X}_{q'} \,\forall\, q' \geqslant q$. Note that $\mathcal{X}_q \subseteq \mathcal{X}_{q'} \,\forall\, q' \geqslant q$. Noting $n_0 = q$, we have that there exists an $x_1 \in V$ such that for all $n \geqslant n_0$, $x_1 \in \mathcal{X}_n$ and $f(x_1) \neq 0$. Furthermore, $0 < \epsilon_0 < \frac{2\pi}{\|f\|_{\infty,[0,1]}}$ implies that $0 < |f(x_1)|\epsilon_0/2 < \pi$ and therefore $\sin^2[f(x_1)\epsilon_0/2] \neq 0$. Finally, as a sum of positive numbers with at least one nonvanishing number, $\|\frac{\hat{I}-e^{-i\hat{f}\epsilon_0}}{2}|s\rangle\|_{2,N} \neq 0 \,\forall\, n \geqslant n_0$, which achieves the proof of Lemma 1. ∎

Lemma 2. For any differentiable function $f \in \mathcal{C}^1([0,1])$ and $\epsilon_1 > 0$, the M Walsh series f^{ϵ_1} defined in Eq. (A2) approximates the function f up to an error $O(\epsilon_1)$:

$$\|f - f^{\epsilon_1}\|_{\infty,[0,1]} \leqslant \epsilon_1 \|f'\|_{\infty,[0,1]}. \tag{B15}$$

Proof. The function f^{ϵ_1} is a sum of M Walsh functions of order $j \in \{0, \dots, M-1\}$. The Walsh function of order j is a piecewise function taking values $+1$ and -1 on at most 2^p different intervals $I_k^p = [k/2^p, (k+1)/2^p[$ with $k \in \{0, \dots, 2^p - 1\}$. The p first terms of the dyadic expansion of all $x \in I_k^p$ are equal. Therefore, the function f^{ϵ_1} is a piecewise function which is constant on each of the $M = 2^m$ intervals I_k^m:

$$f^{\epsilon_1}(x) = f^{\epsilon_1}(k/M) \,\forall\, k \in \{0, \dots, M-1\},\ \forall x \in I_k^m. \tag{B16}$$

Then, from the definitions of f^{ϵ_1} and the Walsh coefficients a_j^f and using the orthonormality of the Walsh functions $\frac{1}{M}\sum_{p=0}^{M-1} w_j(p/M)w_l(p/M) = \delta_{jl}$, we have

$$f^{\epsilon_1}(k/M) = f(k/M). \tag{B17}$$

If we let x be a real number in I_k^m, then $f(x) - f^{\epsilon_1}(x) = f(x) - f(k/M)$. The mean value theorem implies that there exists a $y \in I_k^m$ such that $f(x) - f(k/M) = f'(y)(x - k/M)$. Using $|x - k/M| \leqslant 1/M < \epsilon_1$ and $|f'(y)| \leqslant \|f'\|_{\infty,[0,1]}$, we have

$$|f(x) - f^{\epsilon_1}(x)| \leqslant \|f'\|_{\infty,[0,1]}\epsilon_1 \,\forall\, x \in [0,1]. \tag{B18}$$

∎

Lemma 3. For any function f continuous on [0,1] such that $\|f\|_{\infty,[0,1]} \neq 0$ there exist $n_0 \geqslant 0$ and a constant $C_1 > 0$ such that

$$\|f\|_{2,N} \geqslant C_1\sqrt{N}\,\forall n \geqslant n_0, \tag{B19}$$

with $N = 2^n$.

Proof. The function f is continuous on [0,1] with a nonzero value. The continuity of f and the fact that the dyadic rational numbers are dense in [0,1] imply that there exists an n_0 such that there exists an $x \in [0,1] \cap \mathcal{X}_{n_0}$ such that $f(x) \neq 0$, i.e., for all $n \geqslant n_0$, $x \in \mathcal{X}_n$ and therefore for all $n \geqslant n_0$, $\|f\|_{2,N} \neq 0$ with $N = 2^n$. The sequence $(\frac{1}{\sqrt{N}}\|f\|_{2,N})_N$ can be rewritten using the Riemann sum of $|f|^2$, $(\frac{1}{\sqrt{N}}\|f\|_{2,N})^2 = S_N(|f|^2) = \sum_{k=1}^{N}(\frac{k}{N} - \frac{k-1}{N})|f(x_k)|^2 = \sum_{k=1}^{N}\frac{|f(x_k)|^2}{N}$, which converges toward $\|f\|^2_{2,[0,1]}$. Therefore, $(\frac{1}{\sqrt{N}}\|f\|_{2,N})_N$ converges toward $l = \|f\|_{2,[0,1]} > 0$ and there exists an n_1 such that for all $n \geqslant n_1$, $\frac{1}{\sqrt{2^n}}\|f\|_{2,2^n} > l/2$. By defining $C_1 = \min(\min_{n_0 \leqslant k \leqslant n_1}(\frac{1}{\sqrt{2^k}}\|f\|_{2,2^k}), l/2)$, we have $\|f\|_{2,N} \geqslant C_1\sqrt{N}\,\forall n \geqslant n_0$. ■

Lemma 4. For any function f defined and continuous on [0,1] with $\|f\|_{\infty,[0,1]} \neq 0$, there exists an n_0 such that for all $n \geqslant n_0$ and for all $\epsilon_0 \in]0, \pi/\|f\|_{\infty,[0,1]}]$ the normalization factor $\frac{1}{\|\frac{\hat{I}-e^{-i\hat{f}\epsilon_0}}{2}|s\rangle\|_{2,N}}$ can be bounded as

$$\frac{2\sqrt{N}}{\epsilon_0\|f\|_{2,N}} \leqslant \frac{1}{\|\frac{\hat{I}-e^{-i\hat{f}\epsilon_0}}{2}|s\rangle\|_{2,N}} \leqslant C_0\frac{2\sqrt{N}}{\epsilon_0\|f\|_{2,N}}, \tag{B20}$$

which is equivalent to

$$1 \leqslant \frac{\epsilon_0\|f\|_{2,N}}{2\|\sin(f\epsilon_0/2)\|_{2,N}} \leqslant C_0, \tag{B21}$$

with $N = 2^n$ and $C_0 = \pi/2$.

Proof. Lemma 1 implies that there exists an n_0 such that for all $n > n_0$ and for all $\epsilon_0 \in]0, 2\pi/\|f\|_{\infty,[0,1]}[$, $\|\frac{\hat{I}-e^{-i\hat{f}\epsilon_0}}{2}|s\rangle\|_{2,N} \neq 0$, with $N = 2^n$, ensuring that the quantity $1/\|\frac{\hat{I}-e^{-i\hat{f}\epsilon_0}}{2}|s\rangle\|_{2,N}$ is well defined. The left inequality is trivial using the fact that for all $x \geqslant 0$, $\sin(x) \leqslant x$. For the right inequality, consider $\alpha \in]0,\pi]$ and $\epsilon_0 \in]0, \frac{2(\pi-\alpha)}{\|f\|_{\infty,[0,1]}}]$. Then, due to the fact that the function $x \mapsto \sin(x)/x$ is decreasing on $[0,\pi]$,

$$\begin{aligned}&\frac{\epsilon_0\|f\|_{2,N}}{2\|\sin(f\epsilon_0/2)\|_{2,N}}\\ &\leqslant \frac{\|f\|_{2,N}}{\sqrt{\sum_{x\in\mathcal{X}_n} f(x)^2\frac{\sin^2[f(x)(\pi-\alpha)/\|f\|_{\infty,[0,1]}]}{[f(x)(\pi-\alpha)/\|f\|_{\infty,[0,1]}]^2}}}\\ &\leqslant \frac{\pi-\alpha}{\sin(\pi-\alpha)}.\end{aligned} \tag{B22}$$

Therefore, for $\alpha = \pi/2$, Lemma 4 is proved. ■

Lemma 5. For any function f differentiable on [0,1] with $\|f\|_{\infty,[0,1]} \neq 0$ and $\epsilon_1 > 0$ such that $\|f^{\epsilon_1}\|_{\infty,[0,1]} \neq 0$, where f^{ϵ_1} is the Walsh series defined by Eq. (A2), there exists an n_0 such that for all $n \geqslant n_0$ and for all $\epsilon_0 \in]0, \pi/\|f\|_{\infty,[0,1]}]$,

$$\begin{aligned}&\left|\frac{1}{\|\frac{\hat{I}-e^{-i\hat{f}^{\epsilon_1}\epsilon_0}}{2}|s\rangle\|_{2,N}} - \frac{1}{\|\frac{\hat{I}-e^{-i\hat{f}\epsilon_0}}{2}|s\rangle\|_{2,N}}\right|\\ &\quad\leqslant C_0^2\frac{2N\epsilon_1}{\epsilon_0}\frac{\|f'\|_{\infty,[0,1]}}{\|f\|_{2,N}\|f^{\epsilon_1}\|_{2,N}},\end{aligned} \tag{B23}$$

with $N = 2^n$ and $C_0 = \pi/2$.

Proof. First, Lemma 1 implies that there exists an n_1 such that for all $n \geqslant n_1$, $\|\frac{\hat{I}-e^{-i\hat{f}\epsilon_0}}{2}|s\rangle\|_{2,N} \neq 0$, with $N = 2^n$. Then f^{ϵ_1} is a function defined on [0,1] taking 2^m different values of f on the interval $I_k^m = [k/2^m, (k+1)/2^m[$ for $k \in \{0,\dots,2^m-1\}$, with $m = \lfloor\log_2(1/\epsilon_1)\rfloor + 1$. Therefore, the fact that $\|f^{\epsilon_1}\|_{\infty,[0,1]} \neq 0$ implies that there exists an $x \in \mathcal{X}_m$ such that $f^{\epsilon_1}(x) \neq 0$ and by setting $n_0 = \max(n_1, m)$, one has, for all $n \geqslant n_0$, $\|\frac{\hat{I}-e^{-i\hat{f}^{\epsilon_1}\epsilon_0}}{2}|s\rangle\|_{2,N} \neq 0$ and $\|\frac{\hat{I}-e^{-i\hat{f}\epsilon_0}}{2}|s\rangle\|_{2,N} \neq 0$.

Using the subadditivity of the $\|\cdot\|_{2,N}$-norm, we can show that

$$\begin{aligned}&\left|\frac{1}{\|\frac{\hat{I}-e^{-i\hat{f}^{\epsilon_1}\epsilon_0}}{2}|s\rangle\|_{2,N}} - \frac{1}{\|\frac{\hat{I}-e^{-i\hat{f}\epsilon_0}}{2}|s\rangle\|_{2,N}}\right|\\ &\leqslant \frac{\|(e^{-i\hat{f}\epsilon_0} - e^{-i\hat{f}^{\epsilon_1}\epsilon_0})|s\rangle\|_{2,N}}{2\|\frac{\hat{I}-e^{-i\hat{f}^{\epsilon_1}\epsilon_0}}{2}|s\rangle\|_{2,N}\|\frac{\hat{I}-e^{-i\hat{f}\epsilon_0}}{2}|s\rangle\|_{2,N}}\\ &\leqslant \sqrt{N}\frac{\|\sin[(f-f^{\epsilon_1})\epsilon_0/2]\|_{2,N}}{\|\sin(f\epsilon_0/2)\|_{2,N}\|\sin(f^{\epsilon_1}\epsilon_0/2)\|_{2,N}}\\ &\leqslant N\frac{\|f-f^{\epsilon_1}\|_{\infty,[0,1]}}{\|f\|_{2,N}\|f^{\epsilon_1}\|_{2,N}}\frac{\epsilon_0}{2}\left(\frac{2C_0}{\epsilon_0}\right)^2,\end{aligned} \tag{B24}$$

where $\|f\|_{2,N} \leqslant \sqrt{N}\|f\|_{\infty,N} \leqslant \sqrt{N}\|f\|_{\infty,[0,1]}$ and Lemma 4 have been used for the last inequality. Lemma 2 achieves the proof:

$$N\frac{\|f-f^{\epsilon_1}\|_{\infty,[0,1]}}{\|f\|_{2,N}\|f^{\epsilon_1}\|_{2,N}}\frac{2C_0^2}{\epsilon_0} \leqslant C_0^2\frac{2N\epsilon_1}{\epsilon_0}\frac{\|f'\|_{\infty,[0,1]}}{\|f\|_{2,N}\|f^{\epsilon_1}\|_{2,N}}. \tag{B25}$$

■

Lemma 6. For any function f defined and continuous on [0,1] with $\|f\|_\infty \neq 0$ there exists an integer n_0 such that for all $n \geqslant n_0$ and for all $\epsilon_0 \in [0, \pi/\|f\|_{\infty,[0,1]}]$,

$$\left|\frac{\epsilon_0}{2\sqrt{N}\|\frac{\hat{I}-e^{-i\hat{f}\epsilon_0}}{2}|s\rangle\|_{2,N}} - \frac{1}{\|f\|_{2,N}}\right| \leqslant \frac{C_0\epsilon_0^3}{24}\frac{\|f^3\|_{2,N}}{\|f\|^2_{2,N}}, \tag{B26}$$

with $N = 2^n$ and $C_0 = \pi/2$.

Proof. Using the subadditivity of the $\|\cdot\|_{2,N}$-norm, the inequality for all x real, $x-\sin(x)\leqslant\frac{x^3}{6}$, and Lemma 3,

$$\begin{aligned}\left|\frac{\epsilon_0}{2\sqrt{N}\left\|\frac{\hat{I}-e^{-i\hat{f}\epsilon_0}}{2}\left|s\right\rangle\right\|_{2,N}}-\frac{1}{\|f\|_{2,N}}\right| &= \left|\frac{\epsilon_0}{2\|\sin(f\epsilon_0/2)\|_{2,N}}-\frac{1}{\|f\|_{2,N}}\right|\\ &\leqslant \frac{\|\epsilon_0 f/2-\sin(\epsilon_0 f/2)\|_{2,N}}{\|\sin(f\epsilon_0/2)\|_{2,N}\|f\|_{2,N}}\\ &\leqslant \frac{\epsilon_0^3}{48}\frac{\|f^3\|_{2,N}}{\|\sin(f\epsilon_0/2)\|_{2,N}\|f\|_{2,N}}\\ &\leqslant \frac{C_0\epsilon_0^2}{24}\frac{\|f^3\|_{2,N}}{\|f\|_{2,N}^2}.\end{aligned}\tag{B27}$$

■

Lemma 7. For any function f continuous on [0,1] such that $\|f\|_{\infty,[0,1]}\neq 0$ and for any $\epsilon_1>0$ such that $\|f^{\epsilon_1}\|_{\infty,[0,1]}\neq 0$, where f^{ϵ_1} is the Walsh series defined by Eq. (A2), there exists a $C_1>0$ and there exists an n_0 such that for all $n\geqslant n_0$,

$$\|f^{\epsilon_1}\|_{2,N}\geqslant C_1\sqrt{N},\tag{B28}$$

where $N=2^n$ and f^{ϵ_1} is the Walsh series of f defined in Eq. (A2).

Proof. Let us define $m=\lfloor\log_2(1/\epsilon_1)\rfloor+1$ and $M=2^m$. In addition, $\|f^{\epsilon_1}\|_{\infty,[0,1]}\neq 0$ implies that there exists an $x\in\mathcal{X}_m$ such that $f^{\epsilon_1}(x)=f(x)\neq 0$. Then $\|f^{\epsilon_1}\|_{2,M}=\|f\|_{2,M}\neq 0$. Note that $n_0=\min(\{n,\|f\|_{2,2^n}\neq 0\})\leqslant m$. Lemma 3 on f states that there exists a $C_1>0$ such that for all $n\geqslant n_0$, $\|f\|_{2,N}\geqslant\sqrt{N}C_1$. Letting n be an integer larger than n_0, if $m\geqslant n$, $\|f^{\epsilon_1}\|_{2,N}=\|f\|_{2,N}\geqslant C_1\sqrt{N}$, and if $m\leqslant n$, f^{ϵ_1} takes only M different values of f, implying that $\frac{1}{\sqrt{N}}\|f^{\epsilon_1}\|_{2,N}=\frac{1}{\sqrt{M}}\|f\|_{2,M}\geqslant C_1$ since $m\geqslant n_0$. We conclude that there exists a $C_1>0$ and there exists an n_0 such that for all $n\geqslant n_0$, $\|f^{\epsilon_1}\|_{2,N}\geqslant C_1\sqrt{N}$. ■

b. Proof of Theorem 3

Let us consider a differentiable function f defined on [0,1] such that $\|f\|_{\infty,[0,1]}\neq 0$, $\epsilon_0\in]0,\pi/\|f\|_{\infty,[0,1]}]$, and $\epsilon_1>0$ such that $\|f^{\epsilon_1}\|_{\infty,[0,1]}\neq 0$, where f^{ϵ_1} is the Walsh series of f defined in Eq. (A2). The implemented quantum state after measuring $|1\rangle$ for the ancillary qubit $|q_A\rangle$ is

$$|\psi_{f^{\epsilon_1}}\rangle_{\epsilon_0}=-i\frac{\hat{I}-e^{-i\hat{f}^{\epsilon_1}\epsilon_0}}{2\left\|\frac{\hat{I}-e^{-i\hat{f}^{\epsilon_1}\epsilon_0}}{2}\left|s\right\rangle\right\|_{2,N}}\left|s\right\rangle,\tag{B29}$$

where f^{ϵ_1} is the Walsh series approximating f up to an error $\epsilon_1\|f'\|_\infty$ (Lemma 2).

(i) Distance between the target state and the implemented state. Let us bound the infinite norm of the difference between the implemented quantum state $|\psi_{f^{\epsilon_1}}\rangle_{\epsilon_0}$ and the target quantum state $|f\rangle=\frac{1}{\|f\|_{2,N}}\sum_{x\in\mathcal{X}_n}f(x)|x\rangle$,

$$\begin{aligned}\||\psi_{f^{\epsilon_1}}\rangle_{\epsilon_0}-|f\rangle\|_{\infty,N}\leqslant{}&\||\psi_{f^{\epsilon_1}}\rangle_{\epsilon_0}-|\psi_f\rangle_{\epsilon_0}\|_{\infty,N}\\&+\||\psi_f\rangle_{\epsilon_0}-|f\rangle\|_{\infty,N}.\end{aligned}\tag{B30}$$

Let us start to bound the first term by making the difference of the normalization factors appear,

$$\begin{aligned}&\||\psi_{f^{\epsilon_1}}\rangle_{\epsilon_0}-|\psi_f\rangle_{\epsilon_0}\|_{\infty,N}\\ &=\left\|\left(\frac{\hat{I}-e^{-i\hat{f}^{\epsilon_1}\epsilon_0}}{2\left\|\frac{\hat{I}-e^{-i\hat{f}^{\epsilon_1}\epsilon_0}}{2}\left|s\right\rangle\right\|_{2,N}}-\frac{\hat{I}-e^{-i\hat{f}\epsilon_0}}{2\left\|\frac{\hat{I}-e^{-i\hat{f}\epsilon_0}}{2}\left|s\right\rangle\right\|_{2,N}}\right)\left|s\right\rangle\right\|_{\infty,N}\\ &\leqslant\left|\frac{1}{\left\|\frac{\hat{I}-e^{-i\hat{f}^{\epsilon_1}\epsilon_0}}{2}\left|s\right\rangle\right\|_{2,N}}-\frac{1}{\left\|\frac{\hat{I}-e^{-i\hat{f}\epsilon_0}}{2}\left|s\right\rangle\right\|_{2,N}}\right|\\ &\quad\times\left\|\frac{\hat{I}-e^{-i\hat{f}^{\epsilon_1}\epsilon_0}}{2}\left|s\right\rangle\right\|_{\infty,N}\\ &\quad+\left\|\frac{e^{-i\hat{f}^{\epsilon_1}\epsilon_0}-e^{-i\hat{f}\epsilon_0}}{2\left\|\frac{\hat{I}-e^{-i\hat{f}\epsilon_0}}{2}\left|s\right\rangle\right\|_{2,N}}\left|s\right\rangle\right\|_{\infty,N}\\ &\leqslant\left|\frac{1}{\left\|\frac{\hat{I}-e^{-i\hat{f}^{\epsilon_1}\epsilon_0}}{2}\left|s\right\rangle\right\|_{2,N}}-\frac{1}{\left\|\frac{\hat{I}-e^{-i\hat{f}\epsilon_0}}{2}\left|s\right\rangle\right\|_{2,N}}\right|\\ &\quad\times\frac{1}{\sqrt{N}}\max_{x\in\mathcal{X}_n}|\sin[f^{\epsilon_1}(x)\epsilon_0/2]|\\ &\quad+\frac{1}{\left\|\frac{\hat{I}-e^{-i\hat{f}\epsilon_0}}{2}\left|s\right\rangle\right\|_{2,N}}\frac{1}{\sqrt{N}}\max_{x\in\mathcal{X}_n}\left|\sin\left(\frac{[f^{\epsilon_1}(x)-f(x)]\epsilon_0}{2}\right)\right|\\ &\leqslant C_0^2\sqrt{N}\frac{\|f_0'\|_{\infty,[0,1]}\|f\|_{\infty,[0,1]}}{\|f\|_{2,N}\|f^{\epsilon_1}\|_{2,N}}\epsilon_1+C_0\frac{\|f'\|_{\infty,[0,1]}}{\|f\|_{2,N}}\epsilon_1,\end{aligned}\tag{B31}$$

where in the last inequality we use $|\sin(x)|\leqslant|x|$, $\|f^{\epsilon_1}\|_{\infty,N}\leqslant\|f^{\epsilon_1}\|_{\infty,[0,1]}\leqslant\|f\|_{\infty,N}$, and Lemmas 2, 4, and 5. Lemma 3 and 7 imply that there is a constant B depending only on f such that

$$C_0^2\sqrt{N}\frac{\|f\|_{\infty,[0,1]}}{\|f\|_{2,N}\|f^{\epsilon_1}\|_{2,N}}+C_0\frac{1}{\|f\|_{2,N}}\leqslant\frac{B}{\sqrt{N}},\tag{B32}$$

leading to the following bound on the first term:

$$\||\psi_{f^{\epsilon_1}}\rangle_{\epsilon_0}-|\psi_f\rangle_{\epsilon_0}\|_{\infty,N}\leqslant\frac{B}{\sqrt{N}}\|f'\|_{\infty,[0,1]}\epsilon_1.\tag{B33}$$

The second term in inequality (B30) can also be bounded by using the Taylor expansion of the exponential term $e^{-i\hat{f}\epsilon_0}=\hat{I}-i\hat{f}\epsilon_0+R_1(-i\hat{f}\epsilon_0)$, with $R_1(x)=\sum_{k=2}^{+\infty}\frac{x^k}{k!}$, and by making the difference of the norms appear:

$$\begin{aligned}&\||\psi_f\rangle_{\epsilon_0}-|f\rangle\|_{\infty,N}\\ &=\left\|\left(-i\frac{\hat{I}-[\hat{I}-i\hat{f}\epsilon_0+R_1(-i\hat{f}\epsilon_0)]}{2\left\|\frac{\hat{I}-e^{-i\hat{f}\epsilon_0}}{2}\left|s\right\rangle\right\|_{2,N}}-\frac{\sqrt{N}}{\|f\|_{2,N}}\hat{f}\right)\left|s\right\rangle\right\|_{\infty,N}\\ &\leqslant\left|\frac{\epsilon_0}{2\left\|\frac{\hat{I}-e^{-i\hat{f}\epsilon_0}}{2}\left|s\right\rangle\right\|_{2,N}}-\frac{\sqrt{N}}{\|f\|_{2,N}}\right|\|\hat{f}|s\rangle\|_{\infty,N}\\ &\quad+\frac{\|R_1(-i\hat{f}\epsilon_0)\left|s\right\rangle\|_{\infty,N}}{2\left\|\frac{\hat{I}-e^{-i\hat{f}\epsilon_0}}{2}\left|s\right\rangle\right\|_{2,N}}.\end{aligned}\tag{B34}$$

The Taylor inequality applied on the remainders of the cosinus and sinus functions implies $\|R_1(-i\hat{f}\epsilon_0)|s\rangle\|_{\infty,N} \leqslant \frac{\epsilon_0^2}{2\sqrt{N}}\|f^2\|_{\infty,[0,1]} + \frac{\epsilon_0^3}{6\sqrt{N}}\|f^3\|_{\infty,[0,1]}$ and using Lemmas 3 and 6,

$$\||\psi_f\rangle_{\epsilon_0} - |f\rangle\|_{\infty,N} \leqslant \epsilon_0 \frac{C_0\|f^2\|_{\infty,[0,1]}}{2\|f\|_{2,N}} + \epsilon_0^2\left(\frac{C_0}{48}\frac{\|f^3\|_{2,N}}{\|f\|_{2,N}^2}\|f\|_{\infty,[0,1]} + \frac{C_0\|f^3\|_{\infty,[0,1]}}{6\|f\|_{2,N}}\right). \tag{B35}$$

Using Lemma 3 and the fact that $\epsilon_0 \leqslant \pi/\|f\|_{\infty,[0,1]}$, there is a constant A, depending only f, such that

$$\||\psi_f\rangle_{\epsilon_0} - |f\rangle\|_{\infty,N} \leqslant A\frac{\epsilon_0}{\sqrt{N}}. \tag{B36}$$

We can rewrite the inequality in terms of the L_2-norm, using $\|\cdot\|_{2,N} \leqslant \sqrt{N}\|\cdot\|_{\infty,N}$, to obtain

$$\||\psi_{f^{\epsilon_1}}\rangle_{\epsilon_0} - |f\rangle\|_{2,N} \leqslant A\epsilon_0 + B\|f'\|_{\infty,[0,1]}\epsilon_1. \tag{B37}$$

Let us define the fidelity between the target state and the implemented state $F = |\langle f|\psi_{f^{\epsilon_1}}\rangle_{\epsilon_0}|^2$ and the infidelity $1-F$. We can show that Eq. (B37) implies

$$1 - F \leqslant (A\epsilon_0 + B\|f'\|_{\infty,[0,1]}\epsilon_1)^2, \tag{B38}$$

which concludes that $1 - F = O((\epsilon_0 + \|f'\|_{\infty,[0,1]}\epsilon_1)^2)$.

(ii) Bounds on the probability of success. The probability of measuring the ancilla qubit $|q_A\rangle$ in state $|1\rangle$ with $\epsilon_0 \in]0, \pi/\|f\|_{\infty,[0,1]}]$ and $\epsilon_1 \geqslant 0$ is

$$P(1) = \left\|\frac{\hat{I} - e^{-i\hat{f}^{\epsilon_1}\epsilon_0}}{2}|s\rangle\right\|_{2,N}^2 = \frac{1}{N}\left\|\sin\left(\frac{f^{\epsilon_1}\epsilon_0}{2}\right)\right\|_{2,N}^2. \tag{B39}$$

The upper bound is trivial and comes from the inequality $\sin(x) \leqslant x \,\forall x \geqslant 0$,

$$P(1) \leqslant \frac{\|f^{\epsilon_1}\|_{2,N}^2\epsilon_0^2}{4N} \leqslant \frac{\|f\|_{\infty,[0,1]}^2\epsilon_0^2}{4}, \tag{B40}$$

where one has to use $\|f^{\epsilon_1}\|_{2,N} \leqslant \sqrt{N}\|f^{\epsilon_1}\|_{\infty,N} \leqslant \sqrt{N}\|f\|_{\infty,N} \leqslant \sqrt{N}\|f\|_{\infty,[0,1]}$. The lower bound comes from the fact the function $x \mapsto \text{sinc}(x) = \sin(x)/x$ decreases on $[0, \pi/2]$:

$$\begin{aligned} P(1) &= \frac{1}{N}\sum_{x\in\mathcal{X}_n}\sin^2\left(\frac{f^{\epsilon_1}(x)\epsilon_0}{2}\right) \\ &= \frac{1}{N}\sum_{x\in\mathcal{X}_n}\left(\frac{f^{\epsilon_1}(x)\epsilon_0}{2}\right)^2\text{sinc}^2\left(\frac{f^{\epsilon_1}(x)\epsilon_0}{2}\right) \\ &\geqslant \frac{1}{N}\sum_{x\in\mathcal{X}_n}\left(\frac{f^{\epsilon_1}(x)\epsilon_0}{2}\right)^2\text{sinc}^2\left(\frac{\pi}{2}\right) \\ &\geqslant \frac{\epsilon_0^2}{\pi^2 N}\|f^{\epsilon_1}\|_{2,N}^2. \end{aligned} \tag{B41}$$

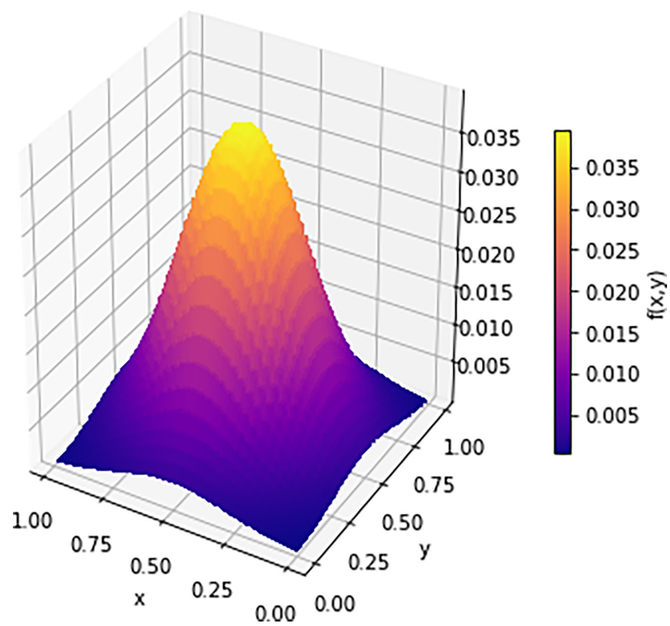

FIG. 10. Two-dimensional quantum state preparation of a two-dimensional Gaussian function $f_2(x, y) = e^{-10[(x-0.5)^2+(y-0.5)^2]}$ on $n = 20$ qubits ($n_x = n_y = 10$) and infidelity $1 - F = 6.2 \times 10^{-3}$ with the parameters $\epsilon_0 = 0.1$ and $\epsilon_{1,x} = \epsilon_{1,y} = 1/2^5$.

Finally, using Lemma 7, there exists a constant D', independent of ϵ_1, such that $\|f_1^\epsilon\|_{2,N}^2 \geqslant ND'$. Therefore, there exists a constant D, independent of ϵ_0, ϵ_1, and N, such that $P(1) \geqslant D\epsilon_0^2$, concluding on $P(1) = \Theta(\epsilon_0^2)$.

(iii) Complexities. The protocol starts with $n+1$ Hadamard gates to prepare the state $|s\rangle = \frac{1}{\sqrt{N}}\sum_{x\in\mathcal{X}_n}|x\rangle$. Then the controlled-$\hat{U}_{f^{\epsilon_1},\epsilon_0}$ operator has asymptotically the same size and depth as the unitary $\hat{U}_{f^{\epsilon_1},\epsilon_0}$ since the controlled operation only changes CNOT gates into Toffoli gates and single-qubit rotations into controlled rotations. The number of single-qubit gates and CNOT gates is $O(M)$, which is also $O(1/\epsilon_1)$. The depth for $\hat{U}_{f^{\epsilon_1},\epsilon_0}$ is also $O(1/\epsilon_1)$ [57]. Finally, a Hadamard gate and phase gate are applied on $|q_A\rangle$ to perform the right interference giving an approximation of the target state up to an infidelity $O((\epsilon_0 + \|f'\|\epsilon_1)^2)$. Therefore, the total size is $O(n + 1/\epsilon_1)$ while the depth is $O(1/\epsilon_1)$. For any function f with values $f(x)$ calculable in time T_f, the number of classical computations to compute the M Walsh coefficients associated with the Walsh series of f is $O(T_f M^2)$, which is also $O(T_f/\epsilon_1^2)$.

4. Multidimensional quantum state preparation

Multidimensional QSP is crucial for many PDEs modeling phenomena appearing in several dimensions. For instance, magnetic fields exists only in spaces with more than two dimensions or kinetic plasma simulations consider the Vlasov-Maxwell equations in two, four, or six dimensions and are particularly challenging to solve even on supercomputers [68]. Quantum algorithms could play a crucial role in overcoming the large computational cost of solving multidimensional PDE problems [24]. In Fig. 10, a bivariate Gaussian is implemented on 20 qubits with a fidelity larger than 0.99.

Definitions. Let us consider the problem of preparing a d-dimensional initial state on $n = n_1 + \cdots + n_d$ qubits, where n_i is the number of qubits associated with the ith axis. We denote by $\mathcal{X}_{n_i}$ the ensemble of $N_i = 2^{n_i}$ positions in [0,1] represented by n_i qubits $\mathcal{X}_{n_i} = \{\sum_{j=0}^{n_i-1} q_j/2^{j+1} \text{ s.t. } q_j \in \{0,1\}\,\forall j\} = \{0, 1/N_i, 2/N_i, 3/N_i, \dots, (N_i-1)/N_i\}$. Let us define $\vec{n} = (n_1, \dots, n_d)$ and $\mathcal{X}_{\vec{n}} = \{(r_1, \dots, r_d) \in \mathcal{X}_{n_1} \times \cdots \times \mathcal{X}_{n_d}\}$. We denote by $|\vec{r}\,\rangle$ the state $|\vec{r}\,\rangle = |r_1\rangle \cdots |r_d\rangle = |r_1\rangle \otimes \cdots \otimes |r_d\rangle \in \mathcal{H}_2^{\otimes n}$.

Let us consider a differentiable real-value function f on $[0,1]^d$ and $\hat{f}$ the associated diagonal operator in the position basis $\{|\vec{r}\,\rangle\}$ such that $\hat{f}|\vec{r}\,\rangle = f(\vec{r}\,)|\vec{r}\,\rangle$. Here $\hat{f}$ encodes the amplitude of the target state $|f\rangle = \sum_{\vec{r}\in\mathcal{X}_{\vec{n}}} f(\vec{r}\,)|r\rangle$. In the multidimensional case, the function f is developed into a Walsh series with respect to each axis i, which gives the equality on the discrete position space for all $\vec{r} \in \mathcal{X}_{\vec{n}}$,

$$f(\vec{r}\,) = \sum_{j_1=0}^{N_1-1} \cdots \sum_{j_d=0}^{N_d-1} a^f_{j_1,\dots,j_d,N_1,\dots,N_d} w_{j_1,\dots,j_d}(\vec{r}\,) = \sum_{\vec{j}=\vec{0}}^{\vec{N}-1} a^f_{\vec{j},\vec{N}} w_{\vec{j}}(\vec{r}\,), \tag{B42}$$

with $w_{j_1,\dots,j_d}(\vec{r}\,) = w_{\vec{j}}(\vec{r}\,) = w_{j_1}(r_1) \times \cdots \times w_{j_d}(r_d)$ and $a^f_{\vec{j},\vec{N}}$ the multidimensional Walsh coefficient

$$a^f_{\vec{j},\vec{N}} = \frac{1}{N} \sum_{\vec{r}\in\mathcal{X}_{\vec{n}}} f(\vec{r}\,) w_{\vec{j}}(\vec{r}\,), \tag{B43}$$

with $N = N_1 \times \cdots \times N_d = 2^{n_1} \times \cdots \times 2^{n_d}$. We denote by $f^{\vec{\epsilon}}$ the approximation of f up to an error $\epsilon = \sum_{i=1}^d \|\partial_i f\|_{\infty,[0,1]^d} \epsilon_i$, with $\epsilon_i > 0$ the error associated with each spatial axis $i \in \{0, \dots, d\}$, defined by

$$f^{\vec{\epsilon}} = \sum_{\vec{j}=\vec{0}}^{\vec{M}-1} a^f_{\vec{j},\vec{M}} w_{\vec{j}}, \tag{B44}$$

where $m_i = \lfloor \log_2(1/\epsilon_i) \rfloor + 1\,\forall i$ and $M_i = 2^{m_i}$ such that $\frac{1}{M_i} < \epsilon_i$. The implemented quantum state after measuring the ancilla qubit $|q_A\rangle = |1\rangle$ is

$$|\psi_{f^{\vec{\epsilon}}}\rangle_{\epsilon_0} = -i \frac{\hat{I} - e^{-i\hat{f}^{\vec{\epsilon}}\epsilon_0}}{2\|\frac{\hat{I}-e^{-i\hat{f}^{\vec{\epsilon}}\epsilon_0}}{2}|s\rangle\|_{2,\vec{N}}} |s\rangle, \tag{B45}$$

where $\epsilon_0 > 0$ and $|s\rangle = \hat{H}^{\otimes n}|0,\dots,0\rangle = \frac{1}{\sqrt{N}} \sum_{\vec{r}\in\mathcal{X}_{\vec{n}}} |\vec{r}\,\rangle$, with $N = N_1 \times \cdots \times N_d$.

Let us define the different multidimensional norms used in this paper. For any vector $|\psi\rangle = \sum_{\vec{r}\in\mathcal{X}_{\vec{n}}} \psi(\vec{r}\,)|\vec{r}\,\rangle \in \mathcal{H}_2^{\otimes n}$,

$$\||\psi\rangle\|_{2,\vec{N}} = \sqrt{\sum_{\vec{r}\in\mathcal{X}_{\vec{n}}} |\psi(\vec{r}\,)|^2}, \tag{B46}$$

$$\||\psi\rangle\|_{\infty,\vec{N}} = \max_{\vec{r}\in\mathcal{X}_{\vec{n}}} |\psi(\vec{r}\,)|, \tag{B47}$$

with $\vec{N} = (N_1, \dots, N_d) = (2^{n_1}, \dots, 2^{n_d})$. For $m_i < n_i\,\forall i$ and $M_i = 2^{m_i}$,

$$\||\psi\rangle\|_{2,\vec{M}} = \sqrt{\sum_{\vec{r}\in\mathcal{X}_{\vec{m}}} |\psi(\vec{r}\,)|^2}. \tag{B48}$$

For any function f defined on $[0,1]^d$,

$$\|f\|_{\infty,[0,1]^d} = \max_{\vec{r}\in[0,1]^d} |f(\vec{r}\,)|, \tag{B49}$$

$$\|f\|_{\infty,\vec{N}} = \max_{\vec{r}\in\mathcal{X}_{\vec{n}}} |f(\vec{r}\,)|, \tag{B50}$$

$$\|f\|_{2,\vec{N}} = \sqrt{\sum_{\vec{r}\in\mathcal{X}_{\vec{n}}} |f(\vec{r}\,)|^2}, \tag{B51}$$

$$\|f\|_{2,[0,1]^d} = \sqrt{\int_{[0,1]^d} |f(\vec{r}\,)|^2 dV}. \tag{B52}$$

Note the following properties:

$$\||\psi\rangle\|_{\infty,\vec{N}} \leqslant \||\psi\rangle\|_{2,\vec{N}} \leqslant \sqrt{N_1 + \cdots + N_d}\||\psi\rangle\|_{\infty,\vec{N}}, \tag{B53}$$

$$\|f\|_{\infty,\vec{N}} \leqslant \|f\|_{2,\vec{N}} \leqslant \sqrt{N_1 + \cdots + N_d}\|f\|_{\infty,\vec{N}}, \tag{B54}$$

$$\|f\|_{\infty,\vec{N}} \leqslant \|f\|_{\infty,[0,1]^d}, \tag{B55}$$

$$\times \frac{1}{\sqrt{N_1 \times \cdots \times N_d}} \|f\|_{2,\vec{N}} \xrightarrow{N_i \to +\infty\,\forall i} \|f\|_{2,[0,1]^d}\ \forall f \in \mathcal{C}_0([0,1]^d). \tag{B56}$$

5. Theorem: Multidimensional case

Let us consider $n_1 + \cdots + n_d$ qubits, a differentiable function f defined on $[0,1]^d$ such that $\|f\|_{\infty,[0,1]^d} \neq 0$, $\epsilon_0 \in]0, \pi/\|f\|_{\infty,[0,1]^d}]$, and $\epsilon_1 > 0, \dots, \epsilon_d > 0$ such that $\|f^{\vec{\epsilon}}\|_{\infty,[0,1]^d} \neq 0$, where $f^{\vec{\epsilon}}$ is the Walsh series of f defined in Eq. (B44).

Theorem 4. There is an efficient quantum circuit of size $O(n_1 + \cdots + n_d + 1/(\epsilon_1 \times \ldots \times \epsilon_d))$ and depth $O(1/(\epsilon_1 \times \cdots \times \epsilon_d))$, which, using one ancillary qubit, implements the quantum state $|f\rangle$ with a probability of success $P(1) = \Theta(\epsilon_0^2)$ and infidelity $1 - F = O((\epsilon_0 + \sum_{i=1}^d \epsilon_i \|\partial_i f\|_{\infty,[0,1]^d})^2)$.

In the particular case of $n_1 = \cdots = n_d = n$ and $\epsilon_0 = \epsilon_1 = \cdots = \epsilon_d$, we can show the following corollary.

Corollary 2. There is an efficient quantum circuit of size $O(nd + 1/\epsilon^{d/2})$ and depth $O(1/\epsilon^{d/2})$, using one ancillary qubit, to implement a quantum state approximating the target state $|f\rangle$ up to an infidelity $1 - F \leqslant \epsilon$ with a probability of success $P(1) = \Theta(\epsilon)$.

For any function f with values $f(\vec{r}\,)$ calculable in time T_f, the number of classical computations needed to find the quantum circuit is $O(T_f/(\epsilon_1 \times \cdots \times \epsilon_d)^2)$ (Theorem 2) or $O(T_f/\epsilon^d)$ (Corollary 2).

6. Proof: Multidimensional case

The proof of Theorem 4 is similar to the proof of Theorem 3. It starts with the following six lemmas.

a. Lemmas

Lemma 8. For any function f continuously defined on $[0,1]^d$ such that $\|f\|_{\infty,[0,1]^d} \neq 0$, there exists an $\vec{n}_0 = (n_{0,1}, \dots, n_{0,d})$ such that for all $n_1 \geqslant n_{0,1}, \dots, n_d \geqslant n_{0,d}$ and for all $\epsilon_0 \in]0, \frac{2\pi}{\|f\|_{\infty,[0,1]^d}}[$, $\|\frac{\hat{I}-e^{-i\hat{f}\epsilon_0}}{2}|s\rangle\|_{2,\vec{N}} \neq 0$, with $\vec{N} = (N_1, \dots, N_d) = (2^{n_1}, \dots, 2^{n_d})$.

Proof. The proof of Lemma 8 is very similar to the proof of Lemma 1. First, the fact that $\|f\|_{\infty,[0,1]^d} \neq 0$ implies that there exists an $\vec{r}_0 \in [0,1]^d$ such that $f(\vec{r}\,) = \|f\|_{\infty,[0,1]^d} \neq 0$.

The continuity of f implies that there exists a neighborhood V of $\vec{r}_0$ such that for all $\vec{r}\in V$, $f(\vec{r})\neq 0$. Note the equality

$$\left\|\frac{\hat{I}-e^{-i\hat{f}\epsilon_0}}{2}\,|s\rangle\right\|_{2,\vec{N}}=\sqrt{\sum_{\vec{r}\in\mathcal{X}_{\vec{n}}}\frac{\sin^2[f(\vec{r})\epsilon_0/2]}{N}},\qquad \text{(B57)}$$

with $N=N_1\times\cdots\times N_d$.

The ensemble $\mathcal{X}_{\vec{n}}=\mathcal{X}_{n_1}\times\cdots\times\mathcal{X}_{n_d}$ is a set of vectors of dyadic rationals. Using the same argument as in the proof of Lemma 1 for each axis, that dyadic rationals are dense in [0,1], there exists a vector $\vec{n}_0=(n_{0,1},\dots,n_{0,d})$ and there exists an $\vec{r}_1\in V$ such that for all $n_1\geqslant n_{1,0},\dots,n_d\geqslant n_{d,0}$, $\vec{r}\in\mathcal{X}_{\vec{n}}$, with $\vec{n}=(n_1,\dots,n_d)$, and $f(\vec{r}_1)\neq 0$.

Furthermore, $0<\epsilon_0<\frac{2\pi}{\|f\|_{\infty,[0,1]^d}}$ implies that $0<|f(\vec{r}_1)|\epsilon_0/2<\pi$ and therefore $\sin^2[f(\vec{r}_1)\epsilon_0/2]\neq 0$. Finally, as a sum of positive numbers with at least one nonvanishing number, for all $n_1\geqslant n_{0,1},\dots,n_d\geqslant n_{0,d}$, $\|\frac{\hat{I}-e^{-i\hat{f}\epsilon_0}}{2}\,|s\rangle\|_{2,\vec{N}}\neq 0$, with $\vec{N}=(N_1,\dots,N_d)=(2^{n_1},\dots,2^{n_d})$, which achieves the proof of Lemma 8. ■

Lemma 9. For any differentiable function $f\in\mathcal{C}^1([0,1]^d)$ and $\epsilon_1>0,\dots,\epsilon_d>0$, the truncated Walsh series $f^{\vec{\epsilon}}$ defined in Eq. (B44) approximates the function f up to an error $O(\epsilon_1+\cdots+\epsilon_d)$,

$$\|f-f^{\vec{\epsilon}}\|_{\infty,[0,1]^d}\leqslant\sum_{i=1}^{d}\epsilon_i\|\partial_i f\|_{\infty,[0,1]^d}.\qquad \text{(B58)}$$

Proof. The proof is similar to the one of Lemma 2. The function $f^{\vec{\epsilon}}$ is a sum of $M=M_1\times\cdots\times M_d$ products of Walsh functions $w_{\vec{j}}(\vec{r})=w_{j_1}(r_1)\times\cdots\times w_{j_d}(r_d)$, with $j_i\in\{0,\dots,M_i-1\}$.

Each Walsh function of order $j_i\leqslant M_i$ is a piecewise function taking values $+1$ and -1 on at most M_i different intervals $I_{k_i}^{m_i}=[k_i/M_i,(k_i+1)/M_i[$ for $k_i\in\{0,\dots,M_i\}$, related to the ith axis. Therefore, $w_{\vec{j}}=w_{j_1}\times\cdots\times w_{j_d}$ and the function $f^{\vec{\epsilon}}$ are piecewise functions constant on the M different volumes $I_{\vec{k}}^{\vec{m}}=I_{k_1}^{m_1}\times\cdots\times I_{k_d}^{m_d}$ with $k_i\in\{0,\dots,M_i\}\,\forall\, i$:

$$f^{\vec{\epsilon}}(\vec{r})=f^{\vec{\epsilon}}(k_1/M_1,\dots,k_d/M_d)\,\forall\vec{k},\ \forall\,\vec{r}\in I_{\vec{k}}^{\vec{m}}.\qquad \text{(B59)}$$

Note that $\vec{r}_{\vec{k},\vec{m}}=(k_1/M_1,\dots,k_d/M_d)$. Then, from the definitions of $f^{\vec{\epsilon}}$ and $a^{f}_{\vec{j},\vec{M}}$ we have

$$f^{\vec{\epsilon}}(\vec{r}_{\vec{k},\vec{m}})=f(\vec{r}_{\vec{k},\vec{m}}).\qquad \text{(B60)}$$

Now let us consider $\vec{r}\in I_{\vec{k}}^{\vec{m}}$ and then $f(\vec{r})-f^{\epsilon_1}(\vec{r})=f(\vec{r})-f(\vec{r}_{\vec{k},\vec{m}})$. Let us consider the curve $\gamma:\left(\begin{smallmatrix}[0,1] & \to & [0,1]^d\\ t & \mapsto & t\vec{r}+(1-t)\vec{r}_{\vec{k},\vec{m}}\end{smallmatrix}\right)$. The mean value theorem on the function $g(t)=f(\gamma(t))$ implies that there exists a $t_1\in[0,1]$ such that $g(1)-g(0)=g'(t_1)(1-0)$, with $g'(t)=\partial_i f(\gamma(t))\gamma'(t)=\sum_{i=1}^d\partial_i f(\gamma(t))(r_i-k_i/M_i)\,\forall\, t\in[0,1]$. Finally, noting that $|r_i-k_i/M_i|\leqslant 1/M_i<\epsilon_i\,\forall\, i$ and $|\partial_i f(\gamma(t))|\leqslant\|\partial_i f\|_{\infty,[0,1]^d}$, we have

$$|f(\vec{r})-f^{\vec{\epsilon}}(\vec{r})|\leqslant\sum_{i=1}^{d}\epsilon_i\|\partial_i f\|_{\infty,[0,1]^d}\,\forall\,\vec{r}\in[0,1]^d.\qquad \text{(B61)}$$

In particular, $\|f-f^{\vec{\epsilon}}\|_{\infty,[0,1]^d}\leqslant\sum_{i=1}^d\epsilon_i\|\partial_i f\|_{\infty,[0,1]^d}$. ■

Lemma 10. For any function f continuously defined on $[0,1]^d$ such that $\|f\|_{\infty,[0,1]^d}\neq 0$ there exists an $\vec{n}_0=(n_{0,1},\dots,n_{0,d})$ such that for all $n_1\geqslant n_{0,1},\dots,n_d\geqslant n_{0,d}$,

$$\|f\|_{2,\vec{N}}\geqslant C_1\sqrt{N},\qquad \text{(B62)}$$

with $N=N_1\times\cdots\times N_d=2^{n_1}\times\cdots\times 2^{n_d}$ and $\vec{N}=(N_1,\dots,N_d)$.

Proof. The function f is continuous on $[0,1]^d$ with a nonzero value. The continuity of f and the fact that the dyadic rational numbers are dense in [0,1] imply that there exists an $\vec{n}_0=(n_{0,1},\dots,n_{0,d})$ such that there exists an $\vec{r}\in[0,1]^d\cap\mathcal{X}_{\vec{n}_0}$ such that $f(\vec{r})\neq\vec{0}$, i.e., for all $n_1\geqslant n_{0,1},\dots,n_d\geqslant n_{0,d}$, $\vec{r}\in\mathcal{X}_{\vec{n}}$, with $\vec{n}=(n_1,\dots,n_d)$, implying that $\|f\|_{2,\vec{N}}\neq 0$ with $\vec{N}=(2^{n_0},\dots,2^{n_d})$ and $\|f\|_{2,[0,1]^d}\neq 0$. The quantity $\frac{1}{\sqrt{N}}\|f\|_{2,\vec{N}}$ can be seen as a Riemann sum over a partition of $[0,1]^d$ composed of subrectangles of volume $1/N$. Therefore, $\frac{1}{\sqrt{N}}\|f\|_{2,\vec{N}}\xrightarrow{N_i\to+\infty\,\forall\, i}\|f\|_{2,[0,1]^d}=l\neq 0$, meaning that for all $\epsilon>0$ there exists an $\vec{n}_1=(n_{1,1},\dots,n_{1,d})$ such that for all $n_1\geqslant n_{1,1},\dots,n_d\geqslant n_{1,d}$, $-\epsilon\leqslant\frac{1}{\sqrt{N}}\|f\|_{2,\vec{N}}-l\leqslant\epsilon$. We conclude the proof by setting $\epsilon=\frac{l}{2}$ such that there exists an $\vec{n}_2=(n_{2,1},\dots,n_{2,d})$ such that for all $n_1\geqslant n_{2,1},\dots,n_d\geqslant n_{2,d}$, $\|f\|_{2,\vec{N}}\geqslant\frac{l}{2}\sqrt{N}$ with $C_1=l/2$. ■

Lemma 11. For any function f defined and continuous on $[0,1]^d$ with $\|f\|_{\infty,[0,1]^d}\neq 0$, there exists an $\vec{n}_0=(n_{0,1},\dots,n_{0,d})$ such that for all $n_1\geqslant n_{0,1},\dots,n_d\geqslant n_{0,d}$ and for all $\epsilon_0\in]0,\pi/\|f\|_{\infty,[0,1]^d}]$ the normalization factor $\frac{1}{\|\frac{\hat{I}-e^{-i\hat{f}\epsilon_0}}{2}|s\rangle\|_{2,\vec{N}}}$ can be bounded as

$$\frac{2\sqrt{N}}{\epsilon_0\|f\|_{2,\vec{N}}}\leqslant\frac{1}{\|\frac{\hat{I}-e^{-i\hat{f}\epsilon_0}}{2}\,|s\rangle\|_{2,\vec{N}}}\leqslant C_0\frac{2\sqrt{N}}{\epsilon_0\|f\|_{2,\vec{N}}},\qquad \text{(B63)}$$

which is equivalent to

$$1\leqslant\frac{\epsilon_0\|f\|_{2,\vec{N}}}{2\|\sin(f\epsilon_0/2)\|_{2,\vec{N}}}\leqslant C_0,\qquad \text{(B64)}$$

with $N=N_1\times\cdots\times N_d=2^{n_1}\times\cdots\times 2^{n_d}$, $\vec{N}=(N_0,\dots,N_d)$, and $C_0=\pi/2$.

Proof. Lemma 8 implies that there exists an $\vec{n}_0=(n_{0,1},\dots,n_{0,d})$ such that for all $n_1\geqslant n_{0,1},\dots,n_d\geqslant n_{0,d}$ and for all $\epsilon_0\in]0,2\pi/\|f\|_{\infty,[0,1]^d}[$, $\|\frac{\hat{I}-e^{-i\hat{f}\epsilon_0}}{2}\,|s\rangle\|_{2,\vec{N}}\neq 0$, with $\vec{N}=(N_0,\dots,N_d)=(2^{n_0},\dots,2^{n_d})$, ensuring that the quantity $1/\|\frac{\hat{I}-e^{-i\hat{f}\epsilon_0}}{2}\,|s\rangle\|_{2,\vec{N}}$ is well defined. The left inequality is trivial using the fact that for all $x\geqslant 0$, $\sin(x)\leqslant x$. For the right inequality, consider $\alpha\in]0,\pi]$ and $\epsilon_0\in]0,\frac{2(\pi-\alpha)}{\|f\|_{\infty,[0,1]^d}}]$. Then, due to the fact that the function sinc : $x\mapsto\sin(x)/x$ decreases on $[0,\pi]$,

$$\begin{aligned}\frac{\epsilon_0\|f\|_{2,\vec{N}}}{2\|\sin(f\epsilon_0/2)\|_{2,\vec{N}}} &\leqslant \frac{\|f\|_{2,\vec{N}}}{\sqrt{\sum_{\vec{r}\in\mathcal{X}_{\vec{n}}} f(\vec{r})^2 \frac{\sin^2[f(\vec{r})(\pi-\alpha)/\|f\|_{\infty,[0,1]^d}]}{[f(\vec{r})(\pi-\alpha)/\|f\|_{\infty,[0,1]^d}]^2}}} \\ &\leqslant \frac{\pi-\alpha}{\sin(\pi-\alpha)}. \end{aligned}\tag{B65}$$

Therefore, for $\alpha=\pi/2$, Lemma 11 is proved. ■

Lemma 12. For any function f differentiable on $[0,1]^d$ with $\|f\|_{\infty,[0,1]^d}\neq 0$ and $\epsilon_1\geqslant 0,\ldots,\epsilon_d\geqslant 0$ such that $\|f^{\vec{\epsilon}}\|_{\infty,[0,1]^d}\neq 0$, where $f^{\vec{\epsilon}}$ is the Walsh series defined by Eq. (B44), there exists an $\vec{n}_0=(n_{0,1},\ldots,n_{0,d})$ such that for all $n_1\geqslant n_{0,1},\ldots,n_d\geqslant n_{0,d}$ and for all $\epsilon_0\in]0,\pi/\|f\|_{\infty,[0,1]^d}]$,

$$\begin{aligned}&\left|\frac{1}{\left\|\frac{\hat{I}-e^{-i\hat{f}^{\vec{\epsilon}}\epsilon_0}}{2}|s\rangle\right\|_{2,\vec{N}}}-\frac{1}{\left\|\frac{\hat{I}-e^{-i\hat{f}\epsilon_0}}{2}|s\rangle\right\|_{2,\vec{N}}}\right| \\ &\quad\leqslant C_0^2\frac{2N}{\epsilon_0\|f\|_{2,\vec{N}}\|f^{\vec{\epsilon}}\|_{2,\vec{N}}}\sum_{i=1}^{d}\epsilon_i\|\partial_i f\|_{\infty,[0,1]^d},\end{aligned}\tag{B66}$$

with $N=N_1\times\cdots\times N_d=2^{n_1}\times\cdots\times 2^{n_d}$ and $C_0=\pi/2$.

Proof. First, Lemma 8 implies that there exists an $\vec{n}_1=(n_{1,1},\ldots,n_{1,d})$ such that for all $n_1\geqslant n_{1,1},\ldots,n_d\geqslant n_{1,d}$ and for all $\epsilon_0\in]0,2\pi/\|f\|_{\infty,[0,1]^d}[$, $\|\frac{\hat{I}-e^{-i\hat{f}\epsilon_0}}{2}|s\rangle\|_{2,\vec{N}}\neq 0$, with $\vec{N}=(N_1,\ldots,N_d)=(2^{n_1},\ldots,2^{n_d})$. Then $f^{\vec{\epsilon}}$ is a function defined on $[0,1]^d$ taking $M=M_1\times\cdots\times M_d=2^{m_1}\times\cdots\times 2^{m_d}$ different values of f on the interval $I^{\vec{m}}_{\vec{k}}=I^{m_1}_{k_1}\times\cdots\times I^{m_d}_{k_d}=[k_1/2^{m_1},(k_1+1)/2^{m_1}[\times\cdots\times[k_d/2^{m_d},(k_d+1)/2^{m_d}[$, with $k_i\in\{0,\ldots,2^{m_i}-1\}\,\forall\, i$ and $m_i=\lfloor\log_2(1/\epsilon_i)\rfloor+1$. Therefore, the fact that $\|f^{\vec{\epsilon}}\|_{\infty,[0,1]^d}\neq 0$ implies that there exists an $\vec{r}\in\mathcal{X}_{\vec{m}}$ such that $f^{\vec{\epsilon}}(\vec{r})\neq 0$ and by setting $\vec{n}_0=(n_{0,1},\ldots,n_{0,d})=(\max(n_{1,1},m_1),\ldots,\max(n_{1,d},m_d))$, we have that for all $n_1\geqslant n_{0,1},\ldots,n_d\geqslant n_{0,d}$, $\|\frac{\hat{I}-e^{-i\hat{f}^{\vec{\epsilon}}\epsilon_0}}{2}|s\rangle\|_{2,\vec{N}}\neq 0$ and $\|\frac{\hat{I}-e^{-i\hat{f}\epsilon_0}}{2}|s\rangle\|_{2,\vec{N}}\neq 0$, with $\vec{N}=(N_0,\ldots,N_d)=(2^{n_1},\ldots,2^{n_d})$.

Using the subadditivity of the $\|\cdot\|_{2,\vec{N}}$-norm, we can show that

$$\begin{aligned}&\left|\frac{1}{\left\|\frac{\hat{I}-e^{-i\hat{f}^{\vec{\epsilon}}\epsilon_0}}{2}|s\rangle\right\|_{2,\vec{N}}}-\frac{1}{\left\|\frac{\hat{I}-e^{-i\hat{f}\epsilon_0}}{2}|s\rangle\right\|_{2,\vec{N}}}\right| \\ &\quad\leqslant\frac{\|(e^{-i\hat{f}\epsilon_0}-e^{-i\hat{f}^{\vec{\epsilon}}\epsilon_0}|s\rangle)\|_{2,\vec{N}}}{2\left\|\frac{\hat{I}-e^{-i\hat{f}^{\vec{\epsilon}}\epsilon_0}}{2}|s\rangle\right\|_{2,\vec{N}}\left\|\frac{\hat{I}-e^{-i\hat{f}\epsilon_0}}{2}|s\rangle\right\|_{2,\vec{N}}} \\ &\quad\leqslant\sqrt{N}\frac{\|\sin[(f-f^{\vec{\epsilon}})\epsilon_0/2]\|_{2,\vec{N}}}{\|\sin(f\epsilon_0/2)\|_{2,\vec{N}}\|\sin(f^{\vec{\epsilon}}\epsilon_0/2)\|_{2,\vec{N}}} \\ &\quad\leqslant N\frac{\|f-f^{\vec{\epsilon}}\|_{\infty,[0,1]^d}}{\|f\|_{2,\vec{N}}\|f^{\vec{\epsilon}}\|_{2,\vec{N}}}\frac{\epsilon_0}{2}\left(\frac{2C_0}{\epsilon_0}\right)^2,\end{aligned}\tag{B67}$$

where, for the last inequality, $\|f\|_{2,\vec{N}}\leqslant\sqrt{N}\|f\|_{\infty,\vec{N}}\leqslant\sqrt{N}\|f\|_{\infty,[0,1]^d}$ and Lemma 11 have been used. Lemma 9 achieves the proof,

$$\begin{aligned}&N\frac{\|f-f^{\epsilon_1}\|_{\infty,[0,1]^d}}{\|f\|_{2,\vec{N}}\|f^{\vec{\epsilon}}\|_{2,\vec{N}}}\frac{2C_0^2}{\epsilon_0} \\ &\quad\leqslant C_0^2\frac{2N}{\epsilon_0\|f\|_{2,\vec{N}}\|f^{\vec{\epsilon}}\|_{2,\vec{N}}}\sum_{i=1}^{d}\epsilon_i\|\partial_i f\|_{\infty,[0,1]^d},\end{aligned}\tag{B68}$$

with $N=N_1\times\cdots\times N_d=2^{n_1}\times\cdots\times 2^{n_d}$ and $C_0=\pi/2$. ■

Lemma 13. For any function f defined and continuous on $[0,1]^d$ with $\|f\|_{\infty,[0,1]^d}\neq 0$ there exists an $\vec{n}_0=(n_{0,1},\ldots,n_{0,d})$ such that for all $n_1\geqslant n_{0,1},\ldots,n_d\geqslant n_{0,d}$ and for all $\epsilon_0\in]0,\pi/\|f\|_{\infty,[0,1]^d}]$,

$$\left|\frac{\epsilon_0}{2\sqrt{N}\left\|\frac{\hat{I}-e^{-i\hat{f}\epsilon_0}}{2}|s\rangle\right\|_{2,\vec{N}}}-\frac{1}{\|f\|_{2,\vec{N}}}\right|\leqslant\frac{C_0\epsilon_0^2}{24}\frac{\|f^3\|_{2,\vec{N}}}{\|f\|^2_{2,\vec{N}}},\tag{B69}$$

with $N=N_1\times\cdots\times N_d=2^{n_1}\times\cdots\times 2^{n_d}$ and $C_0=\pi/2$.

Proof. First, Lemma 8 implies that there exists an $\vec{n}_0=(n_{0,1},\ldots,n_{0,d})$ such that for all $n_1\geqslant n_{0,1},\ldots,n_d\geqslant n_{0,d}$ and for all $\epsilon_0\in]0,\pi/\|f\|_{\infty,[0,1]^d}]$, $\|\frac{\hat{I}-e^{-i\hat{f}\epsilon_0}}{2}|s\rangle\|_{2,\vec{N}}\neq 0$ and $\|f\|_{2,\vec{N}}$, with $\vec{N}=(N_0,\ldots,N_d)=(2^{n_0},\ldots,2^{n_d})$, ensuring that the quantities $1/\|\frac{\hat{I}-e^{-i\hat{f}\epsilon_0}}{2}|s\rangle\|_{2,\vec{N}}$ and $1/\|f\|_{2,\vec{N}}$ are well defined. Using the subadditivity of the $\|\cdot\|_{2,\vec{N}}$-norm, the inequality for all x real, $x-\sin(x)\leqslant\frac{x^3}{6}$, and Lemma 11,

$$\begin{aligned}&\left|\frac{\epsilon_0}{2\sqrt{N}\left\|\frac{\hat{I}-e^{-i\hat{f}\epsilon_0}}{2}|s\rangle\right\|_{2,\vec{N}}}-\frac{1}{\|f\|_{2,\vec{N}}}\right| \\ &\quad=\left|\frac{\epsilon_0}{2\|\sin(f\epsilon_0/2)\|_{2,\vec{N}}}-\frac{1}{\|f\|_{2,\vec{N}}}\right| \\ &\quad\leqslant\frac{\|\epsilon_0 f/2-\sin(\epsilon_0 f/2)\|_{2,\vec{N}}}{\|\sin(f\epsilon_0/2)\|_{2,\vec{N}}\|f\|_{2,\vec{N}}} \\ &\quad\leqslant\frac{\epsilon_0^3}{48}\frac{\|f^3\|_{2,\vec{N}}}{\|\sin(f\epsilon_0/2)\|_{2,\vec{N}}\|f\|_{2,\vec{N}}} \\ &\quad\leqslant\frac{C_0\epsilon_0^2}{24}\frac{\|f^3\|_{2,\vec{N}}}{\|f\|^2_{2,\vec{N}}}.\end{aligned}\tag{B70}$$

■

Lemma 14. For any function f continuous on $[0,1]^d$ such that $\|f\|_{\infty,[0,1]^d}\neq 0$ and $\epsilon_1>0,\ldots,\epsilon_d>0$ such that $\|f^{\vec{\epsilon}}\|_{\infty,[0,1]^d}\neq 0$ there exists a $C_1>0$ and there exists an $\vec{n}_0=(n_{0,1},\ldots,n_{0,d})$ such that for all $n_1\geqslant n_{0,1},\ldots,n_d\geqslant n_{0,d}$,

$$\|f^{\vec{\epsilon}}\|_{2,\vec{N}}\geqslant C_1\sqrt{N},\tag{B71}$$

where $\vec{N}=(2^{n_1},\ldots,2^{n_d})$, $N=N_1\times\cdots\times N_d$, $\vec{\epsilon}=(\epsilon_1,\ldots,\epsilon_d)$, and $f^{\vec{\epsilon}}$ is the Walsh series of f defined in Eq. (B44).

Proof. Let us define, for all $i\in\{1,\ldots,d\}$, $m_i=\lfloor\log_2(1/\epsilon_i)\rfloor+1$ and $M_i=2^{m_i}$. In addition, $\|f^{\vec{\epsilon}}\|_{\infty,[0,1]^d}\neq 0$ implies that there exists an $\vec{r}\in\mathcal{X}_{\vec{m}}$ such that $f^{\vec{\epsilon}}(\vec{r})=f(\vec{r})\neq 0$. Then $\|f^{\vec{\epsilon}}\|_{2,\vec{M}}=\|f\|_{2,\vec{M}}\neq 0$. As shown in the proof of Lemma 8, there exists an $\vec{n}_0=(n_{0,1},\ldots,n_{0,d})$ such that for all $n_1\geqslant n_{0,1},\ldots,n_d\geqslant n_{0,d}$, $\|f\|_{2,\vec{N}}\neq 0$ with $\vec{N}=(2^{n_1},\ldots,2^{n_d})$. Lemma 10 on f states that there exists a $C_1>0$

such that for all $n_1 \geqslant n_{0,1}, \ldots, n_d \geqslant n_{0,d}$, $\|f\|_{2,\vec{N}} \geqslant \sqrt{N}C_1$, with $N = N_1 \times \cdots \times N_d$. Let $\vec{n} = (n_1, \ldots, n_d)$ be a vector such that $n_i \geqslant n_{0,i} \forall i$. Note that if $m_i \geqslant n_i \forall i$, $\|f^{\epsilon_1}\|_{2,\vec{N}} = \|f\|_{2,\vec{N}} \geqslant C_1\sqrt{N}$. Otherwise, we have $\prod_{i=1}^d \frac{1}{\sqrt{N_i}}\|f^{\vec{\epsilon}}\|_{2,\vec{N}} = \prod_{i=1}^d \frac{1}{\sqrt{N_i'}}\|f\|_{2,\vec{N}'} \geqslant C_1$, where $\vec{N}' = (N_0', \ldots, N_d')$ is defined, for all i, as $N_i' = N_i$ if $m_i \geqslant n_i$ and $N_i' = M_i$ if $m_i \leqslant n_i$. We conclude that there exists a $C_1 > 0$ and there exists an $\vec{n}_0$ such that for all $n_1 \geqslant n_{0,1}, \ldots,\ n_d \geqslant n_{0,d}$, $\|f^{\vec{\epsilon}}\|_{2,\vec{N}} \geqslant C_1\sqrt{N}$. ■

b. Proof of Theorem 4

Let us consider $n_1 + \cdots + n_d$ qubits, a differentiable function f defined on $[0,1]^d$ such that $\|f\|_{\infty,[0,1]^d} \neq 0$, $\epsilon_0 \in]0, \pi/\|f\|_{\infty,[0,1]^d}]$, and $\epsilon_1 > 0, \ldots, \epsilon_d > 0$ such that $\|f^{\vec{\epsilon}}\|_{\infty,[0,1]^d} \neq 0$, where $f^{\vec{\epsilon}}$ is the Walsh series of f defined in Eq. (B44). The implemented quantum state after measuring $|1\rangle$ for the ancillary qubit $|q_A\rangle$ is

$$|\psi_{f_0^{\vec{\epsilon}}}\rangle_{\epsilon_0} = -i\frac{\hat{I} - e^{-i\hat{f}_0^{\vec{\epsilon}}\epsilon_0}}{2\left\|\frac{\hat{I}-e^{-i\hat{f}_0^{\vec{\epsilon}}\epsilon_0}}{2}|s\rangle\right\|_{2,\vec{N}}}|s\rangle, \tag{B72}$$

where $f_0^{\vec{\epsilon}}$ is the Walsh series approximating f up to an error $\sum_{i=1}^d \epsilon_i\|\partial_i f\|_{\infty,[0,1]^d}$ (Lemma 9).

(i) Distance between the target state and the implemented state. Let us bound the infinite norm of the difference between the implemented quantum state $|\psi_{f^{\vec{\epsilon}}}\rangle_{\epsilon_0}$ and the target quantum state $|f\rangle = \frac{1}{\|f\|_{2,\vec{N}}}\sum_{\vec{r}\in\mathcal{X}_{\vec{n}}} f(\vec{r})|\vec{r}\rangle$:

$$\||\psi_{f_0^{\vec{\epsilon}}}\rangle_{\epsilon_0} - |f\rangle\|_{\infty,\vec{N}} \leqslant \||\psi_{f_0^{\vec{\epsilon}}}\rangle_{\epsilon_0} - |\psi_f\rangle_{\epsilon_0}\|_{\infty,\vec{N}} + \||\psi_f\rangle_{\epsilon_0} - |f\rangle\|_{\infty,\vec{N}}. \tag{B73}$$

Let us start to bound the first term by making the difference of the normalization factors appear,

$$\begin{aligned}
&\||\psi_{f_0^{\vec{\epsilon}}}\rangle_{\epsilon_0} - |\psi_f\rangle_{\epsilon_0}\|_{\infty,\vec{N}} \\
&= \left\|\frac{\hat{I} - e^{-i\hat{f}_0^{\vec{\epsilon}}\epsilon_0}}{2\left\|\frac{\hat{I}-e^{-i\hat{f}_0^{\vec{\epsilon}}\epsilon_0}}{2}|s\rangle\right\|_{2,\vec{N}}}|s\rangle - \frac{\hat{I} - e^{-i\hat{f}\epsilon_0}}{2\left\|\frac{\hat{I}-e^{-i\hat{f}\epsilon_0}}{2}|s\rangle\right\|_{2,\vec{N}}}|s\rangle\right\|_{\infty,\vec{N}} \\
&\leqslant \left|\frac{1}{\left\|\frac{\hat{I}-e^{-i\hat{f}^{\vec{\epsilon}}\epsilon_0}}{2}|s\rangle\right\|_{2,\vec{N}}} - \frac{1}{\left\|\frac{\hat{I}-e^{-i\hat{f}\epsilon_0}}{2}|s\rangle\right\|_{2,\vec{N}}}\right| \times \left\|\frac{\hat{I} - e^{-i\hat{f}_0^{\vec{\epsilon}}\epsilon_0}}{2}|s\rangle\right\|_{\infty,\vec{N}} \\
&\quad + \left\|\frac{e^{-i\hat{f}^{\vec{\epsilon}}\epsilon_0} - e^{-i\hat{f}\epsilon_0}}{2\left\|\frac{\hat{I}-e^{-i\hat{f}\epsilon_0}}{2}|s\rangle\right\|_{2,\vec{N}}}|s\rangle\right\|_{\infty,\vec{N}} \\
&\leqslant \left|\frac{1}{\left\|\frac{\hat{I}-e^{-i\hat{f}^{\vec{\epsilon}}\epsilon_0}}{2}|s\rangle\right\|_{2,\vec{N}}} - \frac{1}{\left\|\frac{\hat{I}-e^{-i\hat{f}\epsilon_0}}{2}|s\rangle\right\|_{2,\vec{N}}}\right| \times \frac{1}{\sqrt{N}}\max_{\vec{r}\in\mathcal{X}_{\vec{n}}}\left|\sin\left[f_0^{\vec{\epsilon}}(\vec{r})\epsilon_0/2\right]\right| \\
&\quad + \frac{1}{\left\|\frac{\hat{I}-e^{-i\hat{f}\epsilon_0}}{2}|s\rangle\right\|_{2,\vec{N}}}\frac{1}{\sqrt{N}}\max_{\vec{r}\in\mathcal{X}_{\vec{n}}}|\sin\{[f_0^{\vec{\epsilon}}(\vec{r}) - f(\vec{r})]\epsilon_0/2\}| \\
&\leqslant \left(C_0^2\sqrt{N}\frac{\|f\|_{\infty,[0,1]^d}}{\|f\|_{2,\vec{N}}\|f_0^{\vec{\epsilon}}\|_{2,\vec{N}}} + \frac{C_0}{\|f\|_{2,\vec{N}}}\right)\sum_{i=1}^d \epsilon_i\|\partial_i f\|_{\infty,[0,1]^d},
\end{aligned} \tag{B74}$$

where in the last inequality we use $|\sin(x)| \leqslant |x|$, $\|f^{\vec{\epsilon}}\|_{\infty,\vec{N}} \leqslant \|f^{\vec{\epsilon}}\|_{\infty,[0,1]^d} \leqslant \|f\|_{\infty,\vec{N}}$, and Lemmas 9, 11, and 12. Lemmas 10 and 14 imply there is a constant $B > 0$ depending only on f such that

$$C_0^2\sqrt{N}\frac{\|f\|_{\infty,[0,1]^d}}{\|f\|_{2,\vec{N}}\|f_0^{\vec{\epsilon}}\|_{2,\vec{N}}} + C_0\frac{1}{\|f\|_{2,\vec{N}}} \leqslant \frac{B}{\sqrt{N}}, \tag{B75}$$

leading to the bound on the first term

$$\||\psi_{f_0^{\vec{\epsilon}}}\rangle_{\epsilon_0} - |\psi_f\rangle_{\epsilon_0}\|_{\infty,\vec{N}} \leqslant \frac{B}{\sqrt{N}}\sum_{i=1}^d \epsilon_i\|\partial_i f\|_{\infty,[0,1]^d}. \tag{B76}$$

The second term in the inequality (B73) is bounded by using the Taylor expansion of the exponential term $e^{-i\hat{f}\epsilon_0} = \hat{I} - i\hat{f}\epsilon_0 + R_1(-i\hat{f}\epsilon_0)$, with $R_1(x) = \sum_{k=2}^{+\infty}\frac{x^k}{k!}$, and by making the difference of the norms appear:

$$\begin{aligned}
\||\psi_f\rangle_{\epsilon_0} - |f\rangle\|_{\infty,\vec{N}} &= \left\| -i\frac{\hat{I} - [\hat{I} - i\hat{f}\epsilon_0 + R_1(-i\hat{f}\epsilon_0)]}{2\left\|\frac{\hat{I}-e^{-i\hat{f}\epsilon_0}}{2}|s\rangle\right\|_{2,\vec{N}}}|s\rangle - \frac{\sqrt{N}}{\|f\|_{2,\vec{N}}}\hat{f}|s\rangle\right\|_{\infty,\vec{N}} \\
&\leqslant \left|\frac{\epsilon_0}{2\left\|\frac{\hat{I}-e^{-i\hat{f}\epsilon_0}}{2}|s\rangle\right\|_{2,\vec{N}}} - \frac{\sqrt{N}}{\|f\|_{2,\vec{N}}}\right|\|\hat{f}|s\rangle\|_{\infty,\vec{N}} \\
&\quad + \frac{\|R_1(-i\hat{f}\epsilon_0)|s\rangle\|_{\infty,\vec{N}}}{2\left\|\frac{\hat{I}-e^{-i\hat{f}\epsilon_0}}{2}|s\rangle\right\|_{2,\vec{N}}}.
\end{aligned} \tag{B77}$$

The Taylor inequality applied on the remainders of the cosinus and sinus functions implies $\|R_1(-i\hat{f}\epsilon_0)|s\rangle\|_{\infty,\vec{N}} \leqslant \frac{\epsilon_0^2}{2\sqrt{N}}\|f^2\|_{\infty,[0,1]^d} + \frac{\epsilon_0^3}{6\sqrt{N}}\|f^3\|_{\infty,[0,1]^d}$ and using Lemmas 11 and 13,

$$\begin{aligned}
&\||\psi_f\rangle_{\epsilon_0} - |f\rangle\|_{\infty,\vec{N}} \\
&\quad\leqslant \epsilon_0\frac{C_0\|f^2\|_{\infty,[0,1]^d}}{2\|f\|_{2,\vec{N}}} \\
&\qquad + \epsilon_0^2\left(\frac{C_0}{24}\frac{\|f^3\|_{2,\vec{N}}}{\|f\|_{2,\vec{N}}^2}\|f\|_{\infty,[0,1]^d} + \frac{C_0\|f^3\|_{\infty,[0,1]^d}}{6\|f\|_{2,\vec{N}}}\right).
\end{aligned} \tag{B78}$$

Using Lemma 10 and the fact that $\epsilon_0^2 \leqslant \pi\epsilon_0/\|f\|_{\infty,[0,1]^d}$, there is a constant $A > 0$ depending only on f such that

$$\||\psi_f\rangle_{\epsilon_0} - |f\rangle\|_{\infty,\vec{N}} \leqslant A\frac{\epsilon_0}{\sqrt{N}}. \tag{B79}$$

Finally, using the norm inequality $\|\cdot\|_{2,\vec{N}} \leqslant \sqrt{N}\|\cdot\|_{\infty,\vec{N}}$, we get

$$\||\psi_{f^{\vec{\epsilon}}}\rangle_{\epsilon_0} - |f\rangle\|_{2,\vec{N}} \leqslant A\epsilon_0 + B\sum_{i=1}^{d}\epsilon_i\|\partial_i f\|_{\infty,[0,1]^d}. \quad \text{(B80)}$$

This result implies, in terms of the infidelity $1-F = 1 - |\langle f|\psi_{f^{\vec{\epsilon}}}\rangle_{\epsilon_0}|^2$,

$$1 - F \leqslant \left(A\epsilon_0 + B\sum_{i=1}^{d}\epsilon_i\|\partial_i f\|_{\infty,[0,1]^d}\right)^2, \quad \text{(B81)}$$

which concludes that $1 - F = O((\epsilon_0 + \sum_{i=1}^{d}\epsilon_i\|\partial_i f\|_{\infty,[0,1]^d})^2)$.

(ii) Bounds on the probability of success. The probability of measuring the ancilla qubit $|q_A\rangle$ in state $|1\rangle$ with $\epsilon_0 \in]0,\pi/\|f\|_{\infty,[0,1]^d}]$ is

$$P(1) = \left\|\frac{\hat{I} - e^{-i\hat{f}^{\vec{\epsilon}}\epsilon_0}}{2}|s\rangle\right\|_{2,\vec{N}}^2 = \frac{1}{N}\left\|\sin\left(\frac{f^{\vec{\epsilon}}\epsilon_0}{2}\right)\right\|_{2,\vec{N}}^2. \quad \text{(B82)}$$

The upper bound comes from the inequality $\sin(x) \leqslant x\,\forall x \geqslant 0$,

$$P(1) \leqslant \frac{\|f^{\vec{\epsilon}}\|_{2,\vec{N}}^2\epsilon_0^2}{4N} \leqslant \frac{\|f\|_{\infty,[0,1]^d}^2\epsilon_0^2}{4}, \quad \text{(B83)}$$

where we use $\|f^{\vec{\epsilon}}\|_{2,\vec{N}} \leqslant \sqrt{N}\|f^{\vec{\epsilon}}\|_{\infty,\vec{N}} \leqslant \sqrt{N}\|f\|_{\infty,\vec{N}} \leqslant \sqrt{N}\|f\|_{\infty,[0,1]^d}$. The lower bound comes from the fact the function $x \mapsto \mathrm{sinc}(x) = \sin(x)/x$ decreases on $[0,\pi/2]$:

$$\begin{aligned} P(1) &= \frac{1}{N}\sum_{x\in\mathcal{X}_n}\sin^2\left(\frac{f^{\vec{\epsilon}}(x)\epsilon_0}{2}\right) \\ &= \frac{1}{N}\sum_{x\in\mathcal{X}_n}\left(\frac{f^{\vec{\epsilon}}(x)\epsilon_0}{2}\right)^2\mathrm{sinc}^2\left(\frac{f^{\vec{\epsilon}}(x)\epsilon_0}{2}\right) \\ &\geqslant \frac{1}{N}\sum_{x\in\mathcal{X}_n}\left(\frac{f^{\vec{\epsilon}}(x)\epsilon_0}{2}\right)^2\mathrm{sinc}^2\left(\frac{\pi}{2}\right) \\ &\geqslant \frac{\epsilon_0^2}{\pi^2 N}\|f^{\vec{\epsilon}}\|_{2,\vec{N}}^2. \end{aligned} \quad \text{(B84)}$$

Lemma 14 implies that there exists a constant D', independent of $\vec{\epsilon}$, such that $\|f^{\vec{\epsilon}}\|_{2,\vec{N}}^2 \geqslant ND'$. Therefore, there exists a constant D, independent of ϵ_0, $\vec{\epsilon}$, and N, such that $P(1) \geqslant D\epsilon_0^2$. This concludes that $P(1) = \Theta(\epsilon_0^2)$.

(iii) Complexities. The protocol starts with $n_1 + \cdots + n_d + 1$ Hadamard gates to prepare the state $|s\rangle = \frac{1}{\sqrt{N}}\sum_{\vec{r}\in\mathcal{X}_{\vec{n}}|r\rangle}$. The number of single-qubit gates and CNOT gates to implement the diagonal unitary operator $\hat{U}_{f^{\vec{\epsilon}},\epsilon_0}$, and thus the controlled-$\hat{U}_{f^{\vec{\epsilon}},\epsilon_0}$ operator, is $O(\frac{1}{\epsilon_1\times\cdots\times\epsilon_d})$. Finally, a Hadamard gate and phase gate are applied on $|q_A\rangle$ to perform the right interference giving the target state up to an infidelity $1 - F = O((\epsilon_0 + \sum_{i=1}^{d}\epsilon_i\|\partial_i f\|_{\infty,[0,1]^d})^2)$. The size is $O(n_1 + \cdots + n_d + \frac{1}{\epsilon_1\times\cdots\times\epsilon_d})$ while the depth is $\frac{1}{\epsilon_1\times\cdots\times\epsilon_d}$, independent of the number of qubits. In the particular case of $n_1 = \cdots = n_d = n$ and $\epsilon_1 = \cdots = \epsilon_d = \epsilon$, the size becomes $O(nd + \frac{1}{\epsilon^d})$ and the depth $O(\frac{1}{\epsilon^d})$.

For any function f with values $f(\vec{r})$ calculable in time T_f, the number of classical computations to compute the Walsh coefficients of the $\vec{M}$ Walsh series of f, with $\vec{M} = (M_1,\ldots,M_d)$, is $O(T_f(M_1\times\cdots\times M_d)^2)$, which is also $O(\frac{T_f}{(\epsilon_1\times\cdots\times\epsilon_d)^2})$.

7. Sparse Walsh series loader

The sparse Walsh series is an efficient tool to design quantum circuits for quantum state preparation with particularly small depth and size. For some real-value functions of particular interests, Fig. 3 shows that one can obtain quantum circuits with smaller depth than the dense Walsh series loader (Theorem 1) in order to reach the same accuracy. The problem of finding the best sparse Walsh series which approximates the target real-value function is called the minimax series problem [58]. One efficient way to get a sparse Walsh series approximating a function f is to compute the Walsh series of f on M points as written in Eq. (A2). Then one can sort the absolute value of the M coefficients in decreasing order and implement the largest ones once a target infidelity is reached. Other possible methods include threshold sampling, data compression [58], or efficient estimation of the number M of best Walsh coefficients [63].

Definitions. Let us consider the problem of loading to n qubits a sparse Walsh series

$$f_s = \sum_{j\in S}a_j w_j \quad \text{(B85)}$$

with real coefficients a_j, where $S \subseteq \{0,\ldots,2^{n_0}-1\}$, with n_0 an integer such that $n \geqslant n_0$. The sparsity of the Walsh series is defined as the number of terms in the series, i.e., the cardinal of S: $s = |S|$. The complexity of the quantum circuit implementing a sparse Walsh series depends directly on a parameter k defined as the maximum Hamming weight of the binary decomposition of the Walsh coefficient indices: $k = \max_{j\in S}(\sum_{i=0}^{l_j} j_i)$ with $j = \sum_{i=0}^{l_j} j_i 2^i$ and $j_i \in \{0,1\}$. The parameter k is also the maximum number of qubits on which one Walsh operator is implemented, implying that $k \leqslant n_0$.

Theorem 5. Let f_s be a sparse Walsh series with sparsity s and parameters n_0 and k as defined in Eq. (B85) such that $\|f_s\|_{\infty,[0,1]} \neq 0$. Then for all $n \geqslant n_0$ and $\epsilon_0 \in]0,\pi/\|f_s\|_{\infty,[0,1]}]$ there is a quantum circuit of size $O(n+sk)$ and depth $O(sk)$ which, using one ancillary qubit, implements the quantum state $|f_s\rangle = \frac{1}{\|f_s\|_{2,N}}\sum_{x\in\mathcal{X}_n}f_s(x)|x\rangle$ with a probability of success $P(1) = \Theta(\epsilon_0^2)$ and infidelity $1 - F \leqslant \epsilon_0^2$.

We now consider a function f approximated by a sparse Walsh series f_s.

Corollary 3. Let f be a real-value function defined on [0,1] such that $\|f\|_{\infty,[0,1]} \neq 0$ and let f_s be a sparse Walsh series of sparsity s and parameters n_0 and k as defined in Eq. (B85) such that $\|f_s\|_{\infty,[0,1]} \neq 0$ and $\|f - f_s\|_{\infty,[0,1]} \leqslant \epsilon_1$. Then for all $n \geqslant n_0$ and for all $\epsilon_0 \in]0,\pi/\|f_s\|_\infty]$ there is a quantum circuit of size $O(n+sk)$ and depth $O(sk)$ which, using one ancillary qubit, implements the quantum state $|f\rangle = \frac{1}{\|f\|_{2,N}} \sum_{x\in\mathcal{X}_n} f(x)|x\rangle$ with a probability of success $P(1) = \Theta(\epsilon_0^2)$ and infidelity $1 - F \leqslant (\epsilon_0 + \epsilon_1)^2$.

The proof of this theorem and corollary is very similar to the proof of Theorem 3. It is based on the following lemmas.

Lemma 15. For any sparse Walsh series f_s of parameter n_0 as defined in Eq. (B85) such that $\|f_s\|_{\infty,[0,1]} \neq 0$ for all $n \geqslant n_0$ and for all $\epsilon_0 \in]0, \frac{2\pi}{\|f_s\|_{\infty,[0,1]}}[$, $\|\frac{\hat{I}-e^{-i\hat{f}_s\epsilon_0}}{2}|s\rangle\|_{2,N} \neq 0$, with $N = 2^n$.

Proof. The function f_s is a sum of s Walsh functions of order $j \in \{0, \dots, 2^{n_0} - 1\}$. The Walsh function of order j is a piecewise function taking values $+1$ and -1 on at most 2^p different intervals $I_k^p = [k/2^p, (k+1)/2^p[$, with $p \leqslant n_0$ and $k \in \{0, \dots, 2^p - 1\}$. Therefore, the function f_s is a piecewise function which is constant on each of the $N_0 = 2^{n_0}$ intervals $I_k^{n_0}$:

$$f_s(x) = f_s(k/N_0)\,\forall\, k \in \{0, \dots, N_0 - 1\},\ \forall\, x \in I_k^{n_0}. \quad \text{(B86)}$$

The fact that $\|f_s\|_{\infty,[0,1]} \neq 0$ implies that there exists a $k_0 \in \{0, \dots, 2^{n_0} - 1\}$ such that for all $x \in I_{k_0}^{n_0}$, $f_s(x) = \|f_s\|_{\infty,[0,1]} \neq 0$. Note that for all $n \geqslant n_0$, $\mathcal{X}_{n_0} \subseteq \mathcal{X}_n$ and $I_{k_0}^{n_0} \cap \mathcal{X}_{n_0} \neq 0$. Therefore,

$$\left\|\frac{\hat{I} - e^{-i\hat{f}_s\epsilon_0}}{2}|s\rangle\right\|_{2,N} = \sqrt{\sum_{x\in\mathcal{X}_n} \frac{\sin^2[f_s(x)\epsilon_0/2]}{N}} \geqslant \sqrt{\sum_{x\in I_{k_0}^{n_0}\cap\mathcal{X}_{n_0}} \frac{\sin^2[f_s(x)\epsilon_0/2]}{N}} \geqslant \frac{\sin(\|f_s\|_{\infty,[0,1]}\epsilon_0/2)}{\sqrt{N}}. \quad \text{(B87)}$$

Then $0 < \epsilon_0 < \frac{2\pi}{\|f_s\|_{\infty,[0,1]}}$ implies that $0 < \|f_s\|_{\infty,[0,1]}\epsilon_0/2 < \pi$ and therefore $\sin(\|f_s\|_{\infty,[0,1]}\epsilon_0/2) > 0$. Finally, for all $\epsilon_0 \in]0, \frac{2\pi}{\|f_s\|_{\infty,[0,1]}}[$, and for all $n \geqslant n_0$, $\|\frac{\hat{I}-e^{-i\hat{f}_s\epsilon_0}}{2}|s\rangle\|_{2,N} \neq 0$, which achieves the proof of Lemma 15. ■

Lemma 16. For any sparse Walsh series f_s of the parameter n_0 as defined in Eq. (B85) such that $\|f_s\|_{\infty,[0,1]} \neq 0$, there exists a constant $C_1 > 0$ depending only on f_s and n_0 such that, for all $n \geqslant n_0$,

$$\|f_s\|_{2,N} = C_1\sqrt{N}, \quad \text{(B88)}$$

with $N = 2^n$.

Proof. Note that $I_k^{n_0} = [k/N_0, (k+1)/N_0[$, with $k \in \{0, \dots, N_0 - 1\}$ and $N_0 = 2^{n_0}$ such that $\bigcup_{k=0}^{N_0-1} I_k^{n_0} = [0, 1[$, and for all $n \geqslant n_0$, $|I_k^{n_0} \cap \mathcal{X}_n| = N/N_0$, with $N = 2^n$. Then

$$\|f_s\|_{2,N} = \sqrt{\sum_{x\in\mathcal{X}_n} |f_s(x)|^2} = \sqrt{\sum_{k=0}^{N_0-1} \sum_{x\in I_k^{n_0}\cap\mathcal{X}_n} |f_s(x)|^2} = \sqrt{\sum_{k=0}^{N_0-1} |f_s(k/N_0)|^2 \sum_{x\in I_k^{n_0}\cap\mathcal{X}_n} 1} = \sqrt{\sum_{k=0}^{N_0-1} |f_s(k/N_0)|^2 (N/N_0)} = C_1\sqrt{N}, \quad \text{(B89)}$$

with $C_1 = \sqrt{\frac{1}{N_0}\sum_{k=0}^{N_0-1} |f_s(k/N_0)|^2} = \|f_s\|_{2,N_0}/\sqrt{N_0} > \frac{1}{\sqrt{N_0}} \|f_s\|_{\infty,[0,1]} > 0$. ■

Lemma 17. For any sparse Walsh series f_s of parameter n_0 as defined in Eq. (B85) such that $\|f_s\|_{\infty,[0,1]} \neq 0$, for all $n \geqslant n_0$ and for all $\epsilon_0 \in]0, \pi/\|f_s\|_{\infty,[0,1]}]$ the normalization factor $\frac{1}{\|\frac{\hat{I}-e^{-i\hat{f}_s\epsilon_0}}{2}|s\rangle\|_{2,N}}$ can be bounded as

$$\frac{2}{\epsilon_0 C_1} \leqslant \frac{1}{\left\|\frac{\hat{I}-e^{-i\hat{f}_s\epsilon_0}}{2}|s\rangle\right\|_{2,N}} \leqslant \frac{\pi}{\epsilon_0 C_1}, \quad \text{(B90)}$$

which is equivalent to

$$1 \leqslant \frac{\epsilon_0 C_1\sqrt{N}}{2\|\sin(f_s\epsilon_0/2)\|_{2,N}} \leqslant C_0, \quad \text{(B91)}$$

with $N = 2^n$, $C_0 = \pi/2$, and $C_1 = \|f_s\|_{2,N_0}/\sqrt{N_0}$.

Proof. Lemma 15 implies that for all $n > n_0$ and for all $\epsilon_0 \in]0, 2\pi/\|f_s\|_{\infty,[0,1]}[$, $\|\frac{\hat{I}-e^{-i\hat{f}_s\epsilon_0}}{2}|s\rangle\|_{2,N} \neq 0$, with $N = 2^n$, ensuring the quantity $1/\|\frac{\hat{I}-e^{-i\hat{f}_s\epsilon_0}}{2}|s\rangle\|_{2,N}$ is well defined. The left inequality is trivial using the fact that $\sin(x) \leqslant x\,\forall x \geqslant 0$ and Lemma 16. For the right inequality, consider $\alpha \in]0, \pi]$ and $\epsilon_0 \in]0, \frac{2(\pi-\alpha)}{\|f_s\|_{\infty,[0,1]}}]$. Then, due to the fact that the function $x \mapsto \sin(x)/x$ is decreasing on $[0, \pi]$,

$$\frac{\epsilon_0\|f_s\|_{2,N}}{2\|\sin(f_s\epsilon_0/2)\|_{2,N}} \leqslant \frac{\|f_s\|_{2,N}}{\sqrt{\sum_{x\in\mathcal{X}_n} f_s(x)^2 \frac{\sin^2[f_s(x)(\pi-\alpha)/\|f_s\|_{\infty,[0,1]}]}{[f_s(x)(\pi-\alpha)/\|f_s\|_{\infty,[0,1]}]^2}}} \leqslant \frac{\pi - \alpha}{\sin(\pi - \alpha)}. \quad \text{(B92)}$$

Therefore, for $\alpha = \pi/2$ and using Lemma 16, Lemma 17 is proved. ■

Lemma 18. For any sparse Walsh series f_s of the parameter n_0 as defined in Eq. (B85) such that $\|f_s\|_{\infty,[0,1]} \neq 0$, for all $n \geqslant n_0$ and for all $\epsilon_0 \in [0, \pi/\|f_s\|_{\infty,[0,1]}]$,

$$\left|\frac{\epsilon_0}{2\sqrt{N}\left\|\frac{\hat{I}-e^{-i\hat{f}_s\epsilon_0}}{2}|s\rangle\right\|_{2,N}} - \frac{1}{\|f_s\|_{2,N}}\right| \leqslant C_2\epsilon_0^2/\sqrt{N}, \quad \text{(B93)}$$

with $N = 2^n$ and $C_2 = \frac{\pi}{48}\frac{\|f_s^3\|_{2,N_0}}{\|f_s\|_{2,N_0}^2}$.

Proof. Using the subadditivity of the $\|\cdot\|_{2,N}$-norm, the inequality for all x real, $x-\sin(x)\leqslant\frac{x^3}{6}$, and Lemma 16,

$$\begin{aligned}&\left|\frac{\epsilon_0}{2\sqrt{N}\left\|\frac{\hat{I}-e^{-i\hat{f}_s\epsilon_0}}{2}\,|s\rangle\right\|_{2,N}}-\frac{1}{\|f_s\|_{2,N}}\right|\\&=\left|\frac{\epsilon_0}{2\|\sin(f_s\epsilon_0/2)\|_{2,N}}-\frac{1}{\|f_s\|_{2,N}}\right|\\&\leqslant\frac{\|\epsilon_0 f_s/2-\sin(\epsilon_0 f_s/2)\|_{2,N}}{\|\sin(f_s\epsilon_0/2)\|_{2,N}\|f_s\|_{2,N}}\\&\leqslant\frac{\epsilon_0^3}{48}\frac{\|f_s^3\|_{2,N}}{\|\sin(f_s\epsilon_0/2)\|_{2,N}\|f_s\|_{2,N}}\\&\leqslant\frac{C_0\epsilon_0^2}{24}\frac{\|f_s^3\|_{2,N}}{\|f_s\|_{2,N}^2}=C_2\epsilon_0^2/\sqrt{N},\end{aligned}\tag{B94}$$

with $C_2=\frac{C_0}{24}\frac{\|f_s^3\|_{2,N_0}}{\|f_s\|_{2,N_0}^2}$ and $C_0=\pi/2$. ■

a. Proof of Theorem 5

Let us consider $f_s=\sum_{j\in S}a_jw_j$ a sparse Walsh series of the parameters s, n_0, and k. The quantum state implemented by the sparse WSL is

$$|\psi_{f_s}\rangle=-i\frac{\hat{I}-e^{-i\hat{f}_s\epsilon_0}}{2\left\|\frac{\hat{I}-e^{-i\hat{f}_s\epsilon_0}}{2}\,|s\rangle\right\|_2}\,|s\rangle\,,\tag{B95}$$

with $\hat{f}_s=\sum_{x\in\mathcal{X}_n}f_s(x)|x\rangle\langle x|$ and $|f_s\rangle=\frac{1}{\|f_s\|_{2,N}}\sum_{x\in\mathcal{X}_n}f_s(x)|x\rangle$.

First, we can expand the term $e^{-i\hat{f}_s\epsilon_0}=\hat{I}-i\hat{f}_s\epsilon_0+R_1(-i\hat{f}_s\epsilon_0)$, where R_1 is the remainder of the Taylor series of the exponential function. Then

$$\begin{aligned}&\||\psi_{f_s}\rangle_{\epsilon_0}-|f_s\rangle\|_{\infty,N}\\&\leqslant\frac{\|R_1(-i\hat{f}_s\epsilon_0)\,|s\rangle\|_{\infty,[0,1]}}{2\left\|\frac{\hat{I}-e^{-i\hat{f}_s\epsilon_0}}{2}\,|s\rangle\right\|_2}\\&\quad+\left|\frac{\epsilon_0}{2\left\|\frac{\hat{I}-e^{-i\hat{f}_s\epsilon_0}}{2}\,|s\rangle\right\|_2}-\frac{\sqrt{N}}{\|f_s\|_{2,N}}\right|\|\hat{f}_s|s\rangle\|_{\infty,N}.\end{aligned}\tag{B96}$$

The first term can be bounded using the remainders of the cosinus and sinus functions $\|R_1(-i\hat{f}_s\epsilon_0)|s\rangle\|_{\infty,[0,1]}\epsilon_0)\|\leqslant\|R_{\cos}(\hat{f}_s\epsilon_0)|s\rangle\|_{\infty,[0,1]}+\|R_{\sin}(\hat{f}_s\epsilon_0)|s\rangle\|_{\infty,[0,1]}$, and using the Taylor inequality, we have

$$\|R_{\cos}(\hat{f}_s\epsilon_0)|s\rangle\|_{\infty,[0,1]}\leqslant\frac{\epsilon_0^2\left\|f_s^2\right\|_{\infty,[0,1]}}{2\sqrt{N}}\tag{B97}$$

and

$$\|R_{\sin}(\hat{f}_s\epsilon_0)|s\rangle\|_{\infty,[0,1]}\leqslant\frac{\epsilon_0^3\left\|f_s^3\right\|_{\infty,[0,1]}}{6\sqrt{N}}.\tag{B98}$$

Therefore, using Lemma 17, there exists a $C>0$ such that

$$\frac{\|R_1(-i\hat{f}_s\epsilon_0)\,|s\rangle\|_{\infty,[0,1]}}{2\left\|\frac{\hat{I}-e^{-i\hat{f}_s\epsilon_0}}{2}\,|s\rangle\right\|_2}\leqslant C\frac{\epsilon_0}{\sqrt{N}}.\tag{B99}$$

Then, using Lemma 18, the second term is bounded as

$$\begin{aligned}&\left|\frac{\epsilon_0}{2\left\|\frac{\hat{I}-e^{-i\hat{f}_s\epsilon_0}}{2}\,|s\rangle\right\|_2}-\frac{\sqrt{N}}{\|f_s\|_{2,N}}\right|\|\hat{f}_s|s\rangle\|_{\infty,N}\\&\leqslant C_2\epsilon_0^2\|f_s\|_{\infty,[0,1]}/\sqrt{N}\leqslant C'\frac{\epsilon_0}{\sqrt{N}},\end{aligned}\tag{B100}$$

with $C'>0$. Therefore, there exists a $C''>0$ such that for all $n\geqslant n_0$ and for all $\epsilon_0\in[0,\pi/\|f_s\|_{\infty,[0,1]}]$,

$$\||\psi_{f_s}\rangle_{\epsilon_0}-|f_s\rangle\|_{2,N}\leqslant C''\epsilon_0.\tag{B101}$$

Finally, we have $1-F=O(\epsilon_0^2)$.

In the case where the sparse Walsh series f_s approximates a given function f up to an accuracy ϵ_1 such that

$$\|f-f_s\|_{\infty,[0,1]}\leqslant\epsilon_1,\tag{B102}$$

the quantum state $|\psi_{f_s}\rangle_{\epsilon_0}$ approximates the target quantum state $|f\rangle$ up to an error $O((\epsilon_0+\epsilon_1)^2)$ in terms of infidelity,

$$\begin{aligned}\||f_s\rangle-|f\rangle\|_{\infty,N}&=\max_{x\in\mathcal{X}_n}\left|\frac{f_s(x)}{\|f_s\|_{2,N}}-\frac{f(x)}{\|f\|_{2,N}}\right|\\&\leqslant\frac{\|f_s-f\|_{\infty,[0,1]}}{\|f_s\|_{2,N}}+\left|\frac{1}{\|f\|_{2,N}}-\frac{1}{\|f_s\|_{2,N}}\right|\|f\|_{\infty,[0,1]}\\&\leqslant\frac{\epsilon_1}{\|f_s\|_{2,N}}+\frac{\|f-f_s\|_{2,N}}{\|f\|_{2,N}\|f_s\|_{2,N}}\|f\|_{\infty,[0,1]}\\&\leqslant C_3\epsilon_1/\sqrt{N},\end{aligned}\tag{B103}$$

with $C_3>0$. Therefore, $\||\psi_{f_s}\rangle_{\epsilon_0}-|f\rangle\|_{2,N}=O(\epsilon_0+\epsilon_1)$ and the infidelity between $|\psi_{f_s}\rangle_{\epsilon_0}$ and $|f\rangle$ is $1-F=O((\epsilon_0+\epsilon_1)^2)$. The probability of success is bounded as in Theorem 4: $P(1)=\Theta(\epsilon_0^2)$. The complexity to load an (s,k,n_0)-sparse Walsh series is given by the implementation of s controlled Walsh operators. Each of them is composed of at worst $2k$ Toffoli gates and one controlled-R_Z gates making the depth $O(sk)$ and the size $O(n+sk)$ with the n dependence due to the $n+1$ initial Hadamard gates.

APPENDIX C: AMPLITUDE AMPLIFICATION

The Walsh series loader is based on a repeat-until-success scheme with a probability of success $P(1)=\Theta(\epsilon_0^2)$. It is possible to reach $P(1)=O(1)$ by performing an amplitude amplification scheme [69] at the cost of modifying the size to $O(n\log(n)^4\log(1/\epsilon_0)/\epsilon_0+1/\epsilon_0\epsilon_1)$ and the depth to $O(\log(n)^3\log(1/\epsilon_0)/\epsilon_0+1/\epsilon_0\epsilon_1)$ or, using one additional ancilla qubit (borrowed or zeroed), to a size $O(n\log(n)^4/\epsilon_0+1/\epsilon_0\epsilon_1)$ and a depth $O(\log(n)^3/\epsilon_0+1/\epsilon_0\epsilon_1)$. The total time is reduced by a quadratic factor with respect to the parameter ϵ_0, but the size and depth of the associated quantum circuits are larger. In particular, it makes the depth of the WSL dependent on the number of qubits n.

The amplitude amplification scheme on $n+1$ qubits consists of implementing k times the operator $\hat{U}_{\text{tot}}=-\hat{U}_\psi\hat{U}_P$ with the two unitaries

$$\hat{U}_\psi=\hat{I}-2\,|\psi_3\rangle\langle\psi_3|\,,\tag{C1}$$

$$\hat{U}_P=\hat{I}-2\hat{P},\tag{C2}$$

where $|\psi_3\rangle = \frac{\hat{I}+e^{-i\hat{f}^{\epsilon_1}\epsilon_0}}{2}|s\rangle|0\rangle - i\frac{\hat{I}-e^{-i\hat{f}^{\epsilon_1}\epsilon_0}}{2}|s\rangle|1\rangle$, $\hat{P} = \hat{I}_{\text{position}} \otimes |q_A = 1\rangle\langle q_A = 1|$ is the projector on the target subspace, and $\hat{I} = \hat{I}_{\text{position}} \otimes \hat{I}_A$ is the identity on the $n+1$ qubits. The operator $\hat{U}_\psi$ can be simply rewritten as a product of the operator $\hat{U}_3$ defined as $\hat{U}_3 = (\hat{P}_1\hat{H} \otimes \hat{I}_2^{\otimes n})(\text{controlled-}\hat{U}_{f^{\epsilon_1},\epsilon_0})(\hat{H}^{\otimes(n+1)})$, with $\hat{P}_1 = \begin{pmatrix} 1 & 0 \\ 0 & -i \end{pmatrix}$ such that $\hat{U}_3|0\rangle = |\psi_3\rangle$, and an n anticontrolled Pauli Z gate $\Lambda_n(-Z)$ which applies a phase -1 only if all qubits are in state $|0\rangle$:

$$\hat{U}_\psi = \hat{U}_3\Lambda_n(-Z)\hat{U}_3^\dagger. \tag{C3}$$

The operator $\hat{U}_3$ is composed of $n+1$ Hadamard gates, a phase gate, and the diagonal unitary controlled-$\hat{U}_{f^{\epsilon_1},\epsilon_0}$ operator, which is implemented with a quantum circuit of size and depth $O(1/\epsilon_1)$. The $\Lambda_n(-Z)$ unitary can be implemented using a quantum circuit of size $O(n\log(n)^4)$ and polylogarithmic depth $O(\log(n)^3)$ using one zeroed or borrowed ancilla [70]. The second unitary $\hat{U}_P$ simply corresponds to a Pauli Z gate applied on the ancilla qubit $|q_A\rangle$.

Let us define the positive parameter θ such that $\sin(\theta) = \|\frac{\hat{I}-e^{-i\hat{f}^{\epsilon_1}\epsilon_0}}{2}|s\rangle\|_{2,N} = \Theta(\epsilon_0)$ (Appendix B 3 b). We need to apply the operator $\hat{U}_{\text{tot}}^k$ with $k = \lfloor \pi/4\theta \rfloor$ in order to get $P(1) = O(1)$ [69]. Finally, we can show $\theta = \Theta(\epsilon_0)$ from $\sin(\theta) = \Theta(\epsilon_0)$, implying that $k = \Theta(1/\epsilon_0)$. Therefore, the WSL scheme using amplitude amplification has an overall size $O([n\log(n)^4 + 1/\epsilon_1]/\epsilon_0)$ and depth $O([\log(n)^3 + 1/\epsilon_1]/\epsilon_0)$ using one additional ancilla qubit.

[1] J. Biamonte, P. Wittek, N. Pancotti, P. Rebentrost, N. Wiebe, and S. Lloyd, Quantum machine learning, Nature (London) **549**, 195 (2017).

[2] I. Kerenidis, J. Landman, A. Luongo, and A. Prakash, in *Advances in Neural Information Processing Systems 32*, edited by H. Wallach, H. Larochelle, A. Beygelzimer, F. d'Alché-Buc, E. Fox, and R. Garnett (Curran, Red Hook, 2019).

[3] P. Rebentrost, M. Mohseni, and S. Lloyd, Quantum support vector machine for big data classification, Phys. Rev. Lett. **113**, 130503 (2014).

[4] A. Montanaro, Quantum speedup of Monte Carlo methods, Proc. R. Soc. A **471**, 20150301 (2015).

[5] A. N. Chowdhury and R. D. Somma, Quantum algorithms for Gibbs sampling and hitting-time estimation, Quantum Inf. Comput. **17**, 0041 (2017).

[6] M. Szegedy, *Proceedings of the 45th Annual IEEE Symposium on Foundations of Computer Science, Rome, 2004* (IEEE, Piscataway, 2004), pp. 32–41.

[7] N. Stamatopoulos, D. J. Egger, Y. Sun, C. Zoufal, R. Iten, N. Shen, and S. Woerner, Option pricing using quantum computers, Quantum **4**, 291 (2020).

[8] S. Woerner and D. J. Egger, Quantum risk analysis, npj Quantum Inf. **5**, 15 (2019).

[9] C. Feniou, O. Adjoua, B. Claudon, J. Zylberman, E. Giner, and J.-P. Piquemal, Sparse quantum state preparation for strongly correlated systems, J. Phys. Chem. Lett. **15**, 3197 (2023).

[10] G. H. Low and I. L. Chuang, Hamiltonian simulation by qubitization, Quantum **3**, 163 (2019).

[11] A. W. Harrow, A. Hassidim, and S. Lloyd, Quantum algorithm for linear systems of equations, Phys. Rev. Lett. **103**, 150502 (2009).

[12] L. Wossnig, Z. Zhao, and A. Prakash, Quantum linear system algorithm for dense matrices, Phys. Rev. Lett. **120**, 050502 (2018).

[13] D. W. Berry, High-order quantum algorithm for solving linear differential equations, J. Phys. A: Math. Theor. **47**, 105301 (2014).

[14] D. W. Berry, A. M. Childs, A. Ostrander, and G. Wang, Quantum algorithm for linear differential equations with exponentially improved dependence on precision, Commun. Math. Phys. **356**, 1057 (2017).

[15] S. K. Leyton and T. J. Osborne, A quantum algorithm to solve nonlinear differential equations, arXiv:0812.4423).

[16] J.-P. Liu, H. Ø. Kolden, H. K. Krovi, N. F. Loureiro, K. Trivisa, and A. M. Childs, Efficient quantum algorithm for dissipative nonlinear differential equations, Proc. Natl. Acad. Sci. USA **118**, e2026805118 (2021).

[17] S. Lloyd, G. De Palma, C. Gokler, B. Kiani, Z.-W. Liu, M. Marvian, F. Tennie, and T. Palmer, Quantum algorithm for nonlinear differential equations, arXiv:2011.06571.

[18] D. An, D. Fang, S. Jordan, J.-P. Liu, G. H. Low, and J. Wang, Efficient quantum algorithm for nonlinear reaction-diffusion equations and energy estimation, Commun. Math. Phys. **404**, 963 (2023).

[19] P. C. S. Costa, S. Jordan, and A. Ostrander, Quantum algorithm for simulating the wave equation, Phys. Rev. A **99**, 012323 (2019).

[20] Y. Cao, A. Papageorgiou, I. Petras, J. Traub, and S. Kais, Quantum algorithm and circuit design solving the Poisson equation, New J. Phys. **15**, 013021 (2013).

[21] S. Wang, Z. Wang, W. Li, L. Fan, Z. Wei, and Y. Gu, Quantum fast Poisson solver: The algorithm and complete and modular circuit design, Quantum Inf. Process. **19**, 170 (2020).

[22] A. Scherer, B. Valiron, S.-C. Mau, S. Alexander, E. van den Berg, and T. E. Chapuran, Concrete resource analysis of the quantum linear-system algorithm used to compute the electromagnetic scattering cross section of a 2D target, Quantum Inf. Process. **16**, 60 (2017).

[23] A. M. Childs and J.-P. Liu, Quantum spectral methods for differential equations, Commun. Math. Phys. **375**, 1427 (2020).

[24] A. Engel, G. Smith, and S. E. Parker, Quantum algorithm for the Vlasov equation, Phys. Rev. A **100**, 062315 (2019).

[25] F. Oz, O. San, and K. Kara, An efficient quantum partial differential equation solver with Chebyshev points, Sci. Rep. **13**, 7767 (2023).

[26] J. Zylberman, G. Di Molfetta, M. Brachet, N. F. Loureiro, and F. Debbasch, Quantum simulations of hydrodynamics via the Madelung transformation, Phys. Rev. A **106**, 032408 (2022).

[27] A. Shukla and P. Vedula, A hybrid classical-quantum algorithm for solution of nonlinear ordinary differential equations, Appl. Math. Comput. **442**, 127708 (2023).

[28] M. Lubasch, J. Joo, P. Moinier, M. Kiffner, and D. Jaksch, Variational quantum algorithms for nonlinear problems, Phys. Rev. A **101**, 010301(R) (2020).
[29] H.-L. Liu, Y.-S. Wu, L.-C. Wan, S.-J. Pan, S.-J. Qin, F. Gao, and Q.-Y. Wen, Variational quantum algorithm for the poisson equation, Phys. Rev. A **104**, 022418 (2021).
[30] Y. Liu, Z. Chen, C. Shu, S.-C. Chew, B. C. Khoo, X. Zhao, and Y. Cui, Application of a variational hybrid quantum-classical algorithm to heat conduction equation and analysis of time complexity, Phys. Fluids **34**, 117121 (2022).
[31] K. Kubo, Y. O. Nakagawa, S. Endo, and S. Nagayama, Variational quantum simulations of stochastic differential equations, Phys. Rev. A **103**, 052425 (2021).
[32] R. Demirdjian, D. Gunlycke, C. A. Reynolds, J. D. Doyle, and S. Tafur, Variational quantum solutions to the advection–diffusion equation for applications in fluid dynamics, Quantum Inf. Process. **21**, 322 (2022).
[33] P. García-Molina, J. Rodríguez-Mediavilla, and J. J. García-Ripoll, Quantum Fourier analysis for multivariate functions and applications to a class of Schrödinger-type partial differential equations, Phys. Rev. A **105**, 012433 (2022).
[34] B. Zanger, C. B. Mendl, M. Schulz, and M. Schreiber, Quantum algorithms for solving ordinary differential equations via classical integration methods, Quantum **5**, 502 (2021).
[35] P. C. Costa, D. An, Y. R. Sanders, Y. Su, R. Babbush, and D. W. Berry, Optimal scaling quantum linear-systems solver via discrete adiabatic theorem, PRX Quantum **3**, 040303 (2022).
[36] C. B. Góes, T. O. Maciel, G. G. Pollachini, J. P. Salazar, R. G. Cuenca, and E. I. Duzzioni, Qboost for regression problems: solving partial differential equations, Quantum Inf. Process. **22**, 129 (2023).
[37] R. Chandra, N. T. Jacobson, J. E. Moussa, S. H. Frankel, and S. Kais, Quadratic constrained mixed discrete optimization with an adiabatic quantum optimizer, Phys. Rev. A **90**, 012308 (2014).
[38] G. G. Pollachini, J. P. L. C. Salazar, C. B. D. Góes, T. O. Maciel, and E. I. Duzzioni, Hybrid classical-quantum approach to solve the heat equation using quantum annealers, Phys. Rev. A **104**, 032426 (2021).
[39] J. C. Criado and M. Spannowsky, Qade: Solving differential equations on quantum annealers, Quantum Sci. Technol. **8**, 015021 (2022).
[40] S. Greer and D. O'Malley, *SEG Technical Program Expanded Abstracts 2020* (Society of Exploration Geophysicists, Houston, 2020), pp. 2845–2849.
[41] L. Grover and T. Rudolph, Creating superpositions that correspond to efficiently integrable probability distributions, arXiv:quant-ph/0208112.
[42] M. Mottonen, J. J. Vartiainen, V. Bergholm, and M. M. Salomaa, Transformation of quantum states using uniformly controlled rotations, Quantum Inf. Comput. **5**, 467 (2005).
[43] M. Plesch and Č. Brukner, Quantum-state preparation with universal gate decompositions, Phys. Rev. A **83**, 032302 (2011).
[44] X. Sun, G. Tian, S. Yang, P. Yuan, and S. Zhang, Asymptotically optimal circuit depth for quantum state preparation and general unitary synthesis, IEEE Trans. Comput.-Aid. D. **42**, 3301 (2023).
[45] X.-M. Zhang, M.-H. Yung, and X. Yuan, Low-depth quantum state preparation, Phys. Rev. Res. **3**, 043200 (2021).
[46] X.-M. Zhang, T. Li, and X. Yuan, Quantum state preparation with optimal circuit depth: Implementations and applications, Phys. Rev. Lett. **129**, 230504 (2022).
[47] I. F. Araujo, D. K. Park, F. Petruccione, and A. J. da Silva, A divide-and-conquer algorithm for quantum state preparation, Sci. Rep. **11**, 6329 (2021).
[48] K. Nakaji, S. Uno, Y. Suzuki, R. Raymond, T. Onodera, T. Tanaka, H. Tezuka, N. Mitsuda, and N. Yamamoto, Approximate amplitude encoding in shallow parameterized quantum circuits and its application to financial market indicators, Phys. Rev. Res. **4**, 023136 (2022).
[49] C. Zoufal, A. Lucchi, and S. Woerner, Quantum generative adversarial networks for learning and loading random distributions, npj Quantum Inf. **5**, 103 (2019).
[50] M. Cerezo, A. Arrasmith, R. Babbush, S. C. Benjamin, S. Endo, K. Fujii, J. R. McClean, K. Mitarai, X. Yuan, L. Cincio *et al.*, Variational quantum algorithms, Nat. Rev. Phys. **3**, 625 (2021).
[51] J. R. McClean, S. Boixo, V. N. Smelyanskiy, R. Babbush, and H. Neven, Barren plateaus in quantum neural network training landscapes, Nat. Commun. **9**, 4812 (2018).
[52] G. Marin-Sanchez, J. Gonzalez-Conde, and M. Sanz, Quantum algorithms for approximate function loading, Phys. Rev. Res. **5**, 033114 (2023).
[53] M. Moosa, T. Watts, Y. Chen, A. Sarma, and P. L. McMahon, Linear-depth quantum circuits for loading Fourier approximations of arbitrary functions, Quantum Sci. Technol. **9**, 015002 (2023).
[54] A. G. Rattew and B. Koczor, Preparing arbitrary continuous functions in quantum registers with logarithmic complexity, arXiv:2205.00519.
[55] J. L. Walsh, A closed set of normal orthogonal functions, Am. J. Math. **45**, 5 (1923).
[56] S. S. Bullock and I. L. Markov, Asymptotically optimal circuits for arbitrary *n*-qubit diagonal computations, Quantum Inf. Comput. **4**, 27 (2004).
[57] J. Welch, D. Greenbaum, S. Mostame, and A. Aspuru-Guzik, Efficient quantum circuits for diagonal unitaries without ancillas, New J. Phys. **16**, 033040 (2014).
[58] C.-K. Yuen, Function approximation by Walsh series, IEEE Trans. Comput. **C-24**, 590 (1975).
[59] V. V. Shende and I. L. Markov, On the CNOT-cost of TOFFOLI gates, Quantum Inf. Comput. **9**, 461 (2009).
[60] M. A. Nielsen and I. Chuang, *Quantum Computation and Quantum Information* (Cambridge University Press, Cambridge, 2002).
[61] V. Vandaele, S. Martiel, and T. G. de Brugière, Phase polynomials synthesis algorithms for nisq architectures and beyond, Quantum Sci. Technol. **7**, 045027 (2022).
[62] A. Holmes and A. Y. Matsuura, *2020 IEEE International Conference on Quantum Computing and Engineering (QCE), Denver, 2020* (IEEE, Piscataway, 2020), pp. 169–179.
[63] E. Kushilevitz and Y. Mansour, *Proceedings of the Twenty-Third Annual ACM Symposium on Theory of Computing, New Orleans, 1991* (ACM, New York, 1991), pp. 455–464.
[64] A. Kay, Tutorial on the Quantikz package, arXiv:1809.03842.
[65] J. D. Hunter, Matplotlib: A 2D graphics environment, Comput. Sci. Eng. **9**, 90 (2007).

[66] K. G. Beauchamp, *Applications of Walsh and Related Functions, with an Introduction to Sequency Theory* (Academic, New York, 1984), Vol. 2.

[67] F. Debbasch and M. E. Brachet, Relativistic hydrodynamics of semiclassical quantum fluids, Physica D **82**, 255 (1995).

[68] F. Filbet and E. Sonnendrücker, in *Numerical Mathematics and Advanced Applications*, Proceedings of ENUMATH 2001 the 4th European Conference on Numerical Mathematics and Advanced Applications, Ischia, 2001, edited by F. Brezzi, A. Buffa, S. Corsaro, and A. Murli (Springer, Berlin, 2003), pp. 459–468.

[69] G. Brassard, P. Hoyer, M. Mosca, and A. Tapp, Quantum amplitude amplification and estimation, Contemp. Math. **305**, 53 (2002).

[70] B. Claudon, J. Zylberman, C. Feniou, F. Debbasch, A. Peruzzo, and J.-P. Piquemal, Polylogarithmic-depth controlled-NOT gates without ancilla qubits, arXiv:2312.13206.